



Mathematical Modelling of the First HIV/ZIKV Co-infection Cases in Colombia and Brazil

Jhoana P. Romero-Leiton¹ · Idriss Sekkak² · Julien Arino⁴ · Iain Moyles³ · Bouchra Nasri²

Received: 22 September 2023 / Accepted: 11 February 2025 / Published online: 21 March 2025
© The Author(s), under exclusive licence to the Society for Mathematical Biology 2025

Abstract

This paper presents a mathematical model to investigate the co-infection with human immunodeficiency virus (HIV) and Zika virus (ZIKV) in Colombia and Brazil, where the first cases were reported in 2015. The model considers the sexual transmission dynamics of both viruses and vector-host interactions. We begin by exploring the qualitative behaviour of each model separately. We then analyze the dynamics of the co-infection model using the thresholds and results defined separately for each model. The model also considers the impact of intervention strategies, such as personal protection, antiretroviral therapy (ART), and sexual protection (condom use). Using available and assumed parameter values for Colombia and Brazil, the model is calibrated to investigate the long-term co-infection dynamics, the influence of specific parameters, and the potential effect of implementing these intervention strategies on co-infection spread. The study's results revealed that the duration of Zika infection is a critical factor influencing the burden of co-infection cases. Additionally, bed nets and use of

✉ Bouchra Nasri
bouchra.nasri@umontreal.ca

Jhoana P. Romero-Leiton
jhoana.romero@upr.edu

Idriss Sekkak
idriss.sekkak@umontreal.ca

Julien Arino
julien.arino@umanitoba.ca

Iain Moyles
imoyles@yorku.ca

- ¹ Department of Mathematical Sciences, University of Puerto Rico at Mayagüez, Puerto Rico 00681-9018, USA
- ² Département de Médecine Sociale et Préventive, École de Santé Publique de l'Université de Montréal, Montréal, QC H3N 1X9, Canada
- ³ Department of Mathematics and Statistics, York University, 4700 Keele St, North York, ON M3J 1P3, Canada
- ⁴ Department of Mathematics, University of Manitoba, Winnipeg, MB R3T 1E9, Canada

condoms are essential for disease control, while ART is less emphasized due to the cost-effectiveness of condom use.

Keywords Stability · Equilibrium points · Intervention Strategies · Personal protection · Sexual protection · Antiretroviral therapy · Model calibration

1 Introduction

Human immunodeficiency virus (HIV) and Zika virus (ZIKV) are two major public health concerns worldwide, including Latin America and Caribbean countries (Machado-Silva et al. 2019; García et al. 2014). While HIV is a chronic infection that attacks the immune system, ZIKV is transmitted by mosquitoes and can even cause congenital malformations in children, such as Guillain-Barré syndrome (Cao-Lormeau et al. 2016; Oehler et al. 2014; Smith and Mackenzie 2016) and microcephaly (Mlakar et al. 2016; Calvet et al. 2016). If HIV is not promptly treated, it can cause Acquired Immunodeficiency Syndrome (AIDS) (Kabapy et al. 2020). This virus can be transmitted through sexual contact, syringe misuse, and vertically (from mother to child) (Kabapy et al. 2020). HIV/AIDS still has no cure, so treatments seek to lower or reduce the level of virus replication within the host, which consists of several medications, commonly called antiretroviral therapy (ART) (Saltelli et al. 2008). ZIKV, unlike other arboviruses, also presents transmission through sexual contact. Some studies have demonstrated its detection and transmission through semen, urine, and saliva (Atkinson et al. 2016; Gourinat et al. 2015; Khurshid et al. 2019).

Although HIV is not recognized as a zoonotic disease, it has similar specific transmission mechanisms with ZIKV. Both viruses can be transmitted through sexual contact and vertically from mother to fetus. In endemic zones, the sexual transmission route can substantially worsen the vulnerability of both mother and fetus to other sexually transmitted infections, particularly HIV (Rothan et al. 2018). Until now, there have been few cases of ZIKV infection in HIV-infected individuals worldwide. The first documented case of HIV/ZIKV co-infection was confirmed in a 38-year-old patient in a Rio de Janeiro (Brazil) laboratory in 2015 (Calvet et al. 2016). In the same region, a Zika case was reported in an HIV-infected pregnant woman (Brasil et al. 2016; João et al. 2018). The fetus displayed significant abnormalities, consistent with findings from previous studies conducted on pregnant women who contracted the Zika virus in Brazil. This particular case concluded with the fetus's death (Brasil et al. 2016). In 2018, five individuals from the departments of Risaralda and Sucre were reported with HIV/ZIKV co-infection in Colombia (Smith and Mackenzie 2016), who demonstrated effective immune response and management of the virus levels in their bodies to effectively control ZIKV, as compared to those who were only infected with ZIKV (Smith and Mackenzie 2016).

Therefore, additional research is necessary to understand better the interactions with HIV and ZIKV and the impact of this co-infection on the immune response, disease severity, further complications, and control (Rothan et al. 2018; Smith and Mackenzie 2016). It is not yet well understood how HIV infection increases the risk of ZIKV infection and vice-versa, and how this the co-infection affects pregnant women and

fetuses. Nevertheless, laboratory investigations have demonstrated that placental tissues are susceptible to ZIKV infection (Rothan et al. 2018). ZIKV not only causes immunity response problems but also, in the presence of co-infections, causes placental dysfunction (Rothan et al. 2018). In pregnant women especially, ZIKV mainly targets CD14+ monocytes, which leads to an inflammatory responses and immune tolerance (Rothan et al. 2018). However, there are several ways that ZIKV can play a role in HIV infection, especially via cytokines and the activation of CD4+T cells or linking to HIV (Koblichke et al. 2018). Unlike HIV, the relationship between transmission of ZIKV by mother to child and fetal disease infection has not yet been established (Aschengrau et al. 2021). However, even in the presence of ART, severe viral infection is likely to exacerbate the disorder of the immune system for pregnant women with HIV and increase the risk of transmission from mother to child of HIV and ZIKV (Aschengrau et al. 2021). Therefore, the potential interaction with HIV and ZIKV has recently garnered significant attention (Mittal et al. 2017). These interactions can modify infections' epidemiology, pathogenesis, immune response, and therapy. For instance, co-infection can expedite HIV pathogenesis and enhance transmission by boosting viral replication efficiency. Furthermore, ZIKV transmission and infections can potentially cause serious symptoms and conditions for immunocompromised individuals when co-infections occur (Rothan et al. 2018).

Given the potential impact of HIV/ZIKV co-infection on public health, it is crucial to understand the transmission dynamics of these viruses and evaluate the effectiveness of intervention strategies. Mathematical models are useful for understanding and providing insights into public health policy decisions. To our knowledge, there is no evidence of mathematical models studying the co-infection of HIV and ZIKV phenomenon in the literature. Therefore, this study aimed to formulate and analyze an HIV/ZIKV co-infection model, assuming that both viruses are sexually transmitted and ZIKV is also mosquito-transmitted. The analysis of this model is expected to identify important transmission outcomes that would help to design and evaluate different control and prevention strategies to minimize their impact on public health.

The organization of this study is as follows: In Sect. 2, the co-infection model is introduced. Subsequently, Sects. 2.1 and 2.2 present the individual dynamics of the HIV-only and ZIKV-only models, respectively. Section 3 focuses on the analysis of the co-infection model. The optimal control problem is addressed analytically in Sect. 4. Furthermore, in Sect. 5, a case study centred in Colombia and Brazil is presented, whereby the uncontrolled and controlled models are numerically analyzed using data derived from available literature and convenient assumptions. Finally, in Sect. 6, discussion and concluding remarks are provided, covering the modelling approach and its outcomes, as well as limitations, opportunities for further study and open-ended questions.

2 The HIV/ZIKV Mathematical Model Formulation

This model examines two distinct groups: the human (host) and mosquito (vector) populations. Our model was based on the following hypotheses:

Table 1 Description of the state and control variables involved in the models (2)–(35)

Variable	Description
$N(t)$	The total human population at time t
$S(t)$	Susceptible human population at time t
$I_z(t)$	Infected human population with only ZIKV at time t
$I_h(t)$	Infected human population with only HIV at time t
$I_{hz}(t)$	Infected human population with ZIK/HIV at time t
$A(t)$	Infected human population with AIDS at time t
$R(t)$	Recovered human population of ZIKV at time t
$N_m(t)$	The total mosquito population at time t
$S_m(t)$	Susceptible mosquito population at time t
$I_m(t)$	ZIKV-carrying mosquito population at time t
$\eta_1(t)$	Level of use of bed nets or repellents at time t
$\eta_2(t)$	Level of use of antiretroviral therapy (ART) at time t
$\eta_3(t)$	Level of use of condoms at time t

- We considered that Zika transmission follows an SIR structure for humans and an SI structure for mosquitoes. Additionally, HIV is modelled with an SIA structure, where A represents the compartments of individuals with AIDS. We also assume that the probability of individuals with AIDS transmitting HIV or ZIKV sexually is negligible owing to factors such as reduced viral load under treatment and increased awareness and precautions taken by both patients and healthcare providers.
- No disease intervention strategies were incorporated in the initial stage of the model. However, in subsequent sections (see model (35)), three intervention strategies will be explored, including the use of repellents, antiretroviral therapy (ART), and condom use.
- We assumed that a fully susceptible individual can be co-infected with both Zika and HIV in a single sexual interaction with a co-infected individual.
- The Zika recovery rate for a co-infected human is lower than for a human infected with only Zika (Rothan et al. 2018; Aschengrau et al. 2021; Bidokhti et al. 2018) (scaled by the factor ϵ). However, if a co-infected human recovers from Zika infection, it still remain HIV-carrier.

Tables 1 and 2 show and describe all the variables and parameters involved in our mathematical model.

We define the following force of infections:

$$\begin{aligned} \tilde{\beta}_m &= \beta_m \frac{I_m}{N}, & \tilde{\alpha}_m &= \alpha_m \frac{I_z + I_{hz}}{N}, & \tilde{\beta}_z &= \beta_z \frac{I_z + I_{hz}}{N}, & \tilde{\beta}_h &= \beta_h \frac{I_h + I_{hz}}{N} \quad \text{and} \\ \tilde{\beta}_c &= \beta_c \frac{I_{hz}}{N}. \end{aligned} \tag{1}$$

Table 2 Description and dimension of the parameters involved in the model (2)

Parameter	Description	Dimension
Λ	Recruitment of humans	$Pop \times time^{-1}$
β_m	ZIKV infection rate of humans by contact with ZIKV-carrier mosquitoes	$Time^{-1}$
β_z	ZIKV infection rate of humans by contact with humans infected with ZIKV through sexual contact	$Time^{-1}$
β_h	HIV infection rate of humans by contact with humans infected with HIV through sexual contact	$Time^{-1}$
β_c	HIV/ZIKV infection rate of humans by contact with co-infected humans through sexual contact	$Time^{-1}$
$1/\sigma_1$	Mean duration of the HIV-immunodeficiency period	Time
$1/\sigma_2$	Mean duration of the HIV immunodeficiency period in co-infected individuals	Time
$1/\mu$	Human mean lifespan	Time
$1/\mu_z$	Human mean lifespan after contracting Zika	Time
$1/\mu_h$	Human mean lifespan after contracting HIV	Time
$1/\mu_{hz}$	Human mean lifespan after being co-infected	Time
$1/\delta_z$	Mean duration of the Zika infection	Time
ω_1	Transition probability from HIV to HIV/ZIKV co-infection	Dimensionless
ω_2	Transition probability from ZIKV to HIV/ZIKV co-infection	Dimensionless
ϵ	Scaling factor on Zika recovery rate in co-infected individuals	Dimensionless
Λ_m	Recruitment of mosquitoes	$Pop \times time^{-1}$
α_m	ZIKV infection rate of mosquitoes by contact with infected humans with ZIKV	$Time^{-1}$
$1/\mu_m$	Mosquito mean lifespan	Time

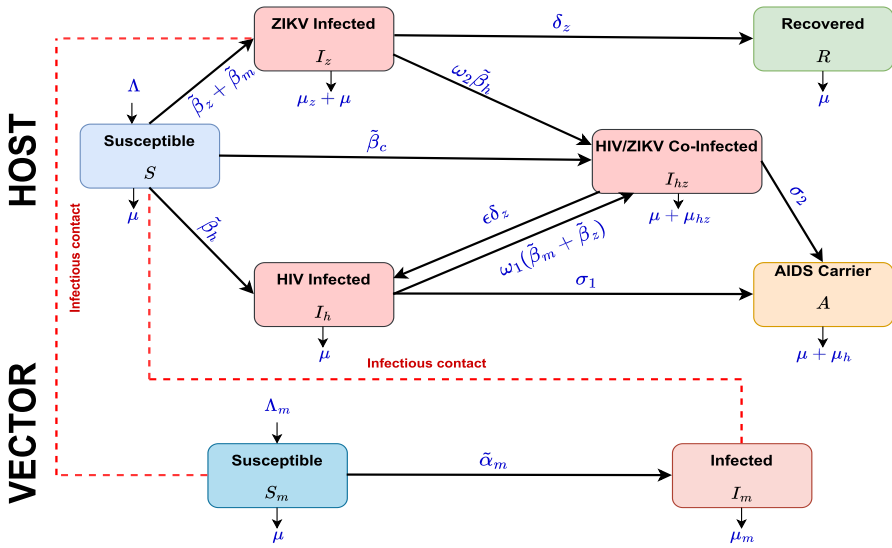


Fig. 1 HIV/ZIKV co-infection model represented in the model (2) (Color figure online)

Then, the mathematical model is described by the following ODEs:

$$\left\{ \begin{aligned} \frac{dS}{dt} &= \Lambda - (\tilde{\beta}_m + \tilde{\beta}_c + \tilde{\beta}_z + \tilde{\beta}_h)S - \mu S \\ \frac{dI_z}{dt} &= (\tilde{\beta}_m + \tilde{\beta}_z)S - \omega_2 \tilde{\beta}_h I_z - (\mu_z + \delta_z + \mu)I_z \\ \frac{dI_h}{dt} &= \epsilon \delta_z I_{hz} + \tilde{\beta}_h S - \omega_1 (\tilde{\beta}_m + \tilde{\beta}_z)I_h - (\sigma_1 + \mu)I_h \\ \frac{dI_{hz}}{dt} &= \tilde{\beta}_c S + \omega_2 \tilde{\beta}_h I_z + \omega_1 (\tilde{\beta}_z + \tilde{\beta}_m)I_h - \epsilon \delta_z I_{hz} - (\sigma_2 + \mu_{hz} + \mu)I_{hz} \\ \frac{dA}{dt} &= \sigma_1 I_h + \sigma_2 I_{hz} - (\mu_h + \mu)A \\ \frac{dR}{dt} &= \delta_z I_z - \mu R \\ \frac{dS_m}{dt} &= \Lambda_m - \tilde{\alpha}_m S_m - \mu_m S_m \\ \frac{dI_m}{dt} &= \tilde{\alpha}_m S_m - \mu_m I_m \end{aligned} \right. \quad (2)$$

Figure 1 illustrates the dynamics represented by the equations involved in the model (2).

In the following two sections, we qualitatively analyze the properties of the system (2). We will start by analyzing the dynamics of the two-component models: the HIV/AIDS model and the ZIKV model.

2.1 Qualitative Behaviour of the HIV/AIDS Model

The HIV/AIDS model is obtained by setting $I_z = I_{hz} = R = S_m = I_m = 0$ in the system (2). Thus, the ODEs described in (2) can be rewritten as:

$$\begin{cases} \frac{dS}{dt} = \Lambda - \beta_h \frac{I_h}{N_h} S - \mu S \\ \frac{dI_h}{dt} = \beta_h \frac{I_h}{N_h} S - (\sigma_1 + \mu) I_h \\ \frac{dA}{dt} = \sigma_1 I_h - (\mu_h + \mu) A, \end{cases} \tag{3}$$

where the total human population is $N_h(t) = S(t) + I_h(t) + A(t)$. For this model, our region of biological interest is

$$\Omega_h = \left\{ (S, I_h, A) \in \mathbb{R}_+^3 : 0 \leq N_h \leq \frac{\Lambda}{\mu} \right\}. \tag{4}$$

It can be proved that Ω_h is positively-invariant under the flow of (3) (see e.g., Romero-Leiton et al. 2019), that is, all solutions of the system (3) starting in Ω_h remain in Ω_h for all $t \geq 0$. Therefore, it is enough to consider the dynamics of (3) in Ω_h .

For our HIV/AIDS model, the disease-free equilibrium (DFE) was analyzed to determine the stability of the system and the potential for an outbreak. For the model (3), the DFE is given by:

$$E_{h_0} = \left(\frac{\Lambda}{\mu}, 0, 0 \right). \tag{5}$$

Here, $\frac{\Lambda}{\mu}$ represents the equilibrium population size when no individuals are infected $I_h = 0$ and $A = 0$. The stability of this equilibrium point can be analyzed in terms of the basic reproduction number for the HIV/AIDS model (\mathcal{R}_h), which can be computed using the next-generation operator (Driessche and Watmough 2002). Using the notation of (Romero-Leiton et al. 2019) in the model (3) the matrices \mathbf{F} (representing the rate of new infections) and \mathbf{V} (representing the rate of transfer between different compartments) are given by

$$\mathbf{F} = \begin{bmatrix} \beta_h & 0 \\ 0 & 0 \end{bmatrix}, \quad \text{and} \quad \mathbf{V} = \begin{bmatrix} \sigma_1 + \mu & 0 \\ -\sigma_1 & \mu_h + \mu \end{bmatrix}.$$

Therefore, to find \mathcal{R}_h , we need to compute the spectral radius, ρ of the matrix \mathbf{FV}^{-1} which corresponds to its largest eigenvalues. This yields,

$$\mathcal{R}_h := \rho(\mathbf{FV}^{-1}) = \frac{\beta_h}{\sigma_1 + \mu}. \tag{6}$$

The basic reproduction number \mathcal{R}_h quantifies the average number of new infections caused by a single infected individual in a fully susceptible population. If $\mathcal{R}_h > 1$,

the DFE is unstable and the disease can potentially spread in the population, leading to an epidemic.

To determine the endemic equilibrium points of the model (3), we must solve the system of algebraic equations

$$\begin{cases} 0 = \Lambda - \beta_h \frac{I_h}{N_h} S - \mu S \\ 0 = \beta_h \frac{I_h}{N_h} S - (\sigma_1 + \mu) I_h \\ 0 = \sigma_1 I_h - (\mu_h + \mu) A. \end{cases} \tag{7}$$

After some algebraic manipulations, and for $I_h, A \neq 0$, we find that the solutions of the system (7) are

$$\begin{aligned} S^* &= \frac{\Lambda \mu (\mu_h + \mu + \sigma)^2}{1 + \mu (\mu + \mu_h + \sigma) (\mu_h + \mu) (\sigma_1 + \mu) (\mathcal{R}_h - 1)}, \\ I_h^* &= \frac{\mu_h + \mu}{\mu_h + \mu + \sigma} (\mathcal{R}_h - 1) S^*, \\ A^* &= \frac{\sigma_1}{\mu_h + \mu + \sigma} (\mathcal{R}_h - 1) S^*. \end{aligned}$$

Thus, as long as $\mathcal{R}_h > 1$, the system (3) has an endemic equilibrium point given by

$$\mathbf{E}_h^* = \left(\frac{\Lambda \mu (\mu_h + \mu + \sigma)^2}{1 + \mu (\mu + \mu_h + \sigma) (\mu_h + \mu) (\sigma_1 + \mu) (\mathcal{R}_h - 1)}, \frac{\mu_h + \mu}{\mu_h + \mu + \sigma} (\mathcal{R}_h - 1) S^*, \frac{\sigma_1}{\mu_h + \mu + \sigma} (\mathcal{R}_h - 1) S^* \right). \tag{8}$$

The following proposition states the global stability of \mathbf{E}_{h_0} and \mathbf{E}_h^* .

Proposition 1 *The system (3) always has a DFE \mathbf{E}_{h_0} given in (5), and for $\mathcal{R}_h > 1$, an endemic equilibrium point \mathbf{E}_h^* given in (8) exists. Additionally,*

- (i) *If $\mathcal{R}_h < 1$, the DFE \mathbf{E}_{h_0} is globally asymptotically stable (GAS), whereas \mathbf{E}_h^* is unstable.*
- (ii) *If $\mathcal{R}_h > 1$, the endemic equilibrium point \mathbf{E}_h^* is GAS, whereas the DFE \mathbf{E}_{h_0} becomes unstable.*

Proof (i) Let $\mathbf{X} = (S, I_h, A)$ and $F(\mathbf{X})$ be the vector field given by the right side hand of the system (3). Additionally, let $\mathbf{Y} = \mathbf{X} + \mathbf{E}_{h_0}$ and define $f(\mathbf{Y}) = F(\mathbf{Y}) - F(\mathbf{E}_{h_0})$ so that $\mathbf{Y} = \mathbf{0}$ is a solution to $\dot{\mathbf{Y}} = f(\mathbf{Y})$. Let us consider the function

$$V(\mathbf{Y}) = \frac{I_h}{\sigma_1 + \mu} \tag{9}$$

noting that $V(\mathbf{0}) = 0$ and $V > 0$ for all $(S, I_h, A) \neq \mathbf{E}_{h_0}$ in Ω_h defined by (4). The orbital derivative of (9) is

$$\dot{V} = \frac{\partial V}{\partial I_h} \dot{I}_h \tag{10}$$

$$= \frac{I_h}{\sigma_1 + \mu} \left(\frac{\beta_h S}{N} - \sigma_1 - \mu \right) \tag{11}$$

$$\leq (\mathcal{R}_h - 1)I_h \leq 0, \tag{12}$$

for all $I_h \geq 0$ when $\mathcal{R}_h \leq 1$. Since $\mathbf{Y} = \mathbf{0}$ is the only trajectory when $I_h = 0$ then by LaSalle’s invariance principle (Hainzl et al. 2022), \mathbf{E}_{h_0} is a global attractor whenever $\mathcal{R}_h < 1$.

- (ii) The third equation of the system (3) is uncoupled in the variable S and its only equilibrium solution is $I_h = \frac{\mu_h + \mu}{\sigma_1} A$. Replacing this value in the first two equations of (3), we obtain the planar system:

$$\begin{cases} \frac{dS}{dt} = \Lambda - \frac{\beta_h(\mu_h + \mu)}{\sigma_1 S + (\mu_h + \mu + \sigma_1)A} AS - \mu S \\ \frac{dA}{dt} = \frac{\beta_h \sigma_1}{\sigma_1 S + (\mu_h + \mu + \sigma_1)A} AS - (\sigma_1 + \mu)A. \end{cases} \tag{13}$$

Therefore, the solutions of the system (3) tend asymptotically to those of the planar system (13) (see e.g. Castillo-Chavez and Thieme 1994). The Dulac criterion (McCluskey and Muldowney 1998) claims that if there exists a real continuously differentiable function $\phi(S, A)$ such that $\nabla \cdot [\phi(S, A)\mathbf{X}(S, A)] \neq 0$, where $\mathbf{X}(S, A) = (F(S, A), G(S, A))$ is the right side hand of system (13), then there are no periodic orbits contained entirely inside Ω_h . Let

$$\phi(S, A) = \frac{\sigma_1 S + (\mu + \mu_h + \sigma_1)A}{SA} \quad \text{for } S > 0, A > 0,$$

then

$$\begin{aligned} \nabla \cdot [\phi(S, A)\mathbf{X}(S, A)] &= \frac{\partial(F\phi)}{\partial S} + \frac{\partial(G\phi)}{\partial A} \\ &= \frac{\partial}{\partial S} \left(\frac{\Lambda(\mu + \mu_h + \sigma_1)}{S} - \frac{\mu\sigma_1 S}{A} \right) - \frac{\partial}{\partial A} \left(\frac{\sigma_1(\mu + \mu_h + \sigma_1)A}{S} + \frac{\mu(\mu + \mu_h + \sigma_1)A}{S} \right) \\ &= - \left(\frac{\Lambda(\mu + \mu_h + \sigma_1)}{S^2} + \frac{\mu\sigma_1}{A} + \frac{(\mu + \mu_h + \sigma_1)(\mu + \sigma_1)}{S} \right) < 0, \text{ for } S, A > 0. \end{aligned}$$

Thus, there are no periodic orbits in Ω_h . Given that Ω_h is positively invariant, and the endemic equilibrium exists if $\mathcal{R}_h > 1$, it follows from the Poincaré-Bendixson Theorem (McCluskey and Muldowney 1998) that all solutions of the system starting in Ω_h remain in Ω_h for all t . Thus, because of the absence of periodic orbits in Ω_h , this implies that the unique endemic equilibrium of the system (3) is GAS when $\mathcal{R}_h > 1$.

□

2.2 Qualitative Behaviour of the ZIKV Model

By setting $I_h = I_{hz} = A = 0$ in the system (2), we obtain the ZIKV model as follows

$$\begin{cases} \frac{dS}{dt} = \Lambda - \left(\beta_m \frac{I_m}{N_z} + \beta_z \frac{I_z}{N_z} \right) S - \mu S \\ \frac{dI_z}{dt} = \left(\beta_m \frac{I_m}{N_z} + \beta_z \frac{I_z}{N_z} \right) S - (\mu_z + \delta_z + \mu) I_z \\ \frac{dR}{dt} = \delta_z I_z - \mu R \\ \frac{dS_m}{dt} = \Lambda_m - \alpha_m \frac{I_z}{N_z} S_m - \mu_m S_m \\ \frac{dI_m}{dt} = \alpha_m \frac{I_z}{N_z} S_m - \mu_m I_m \end{cases} \tag{14}$$

For this model, the total human population is $N_z(t) = S(t) + I_z(t) + R(t)$, and the total mosquito population is $N_m(t) = S_m(t) + I_m(t)$. We are interested in analyzing the solutions within the biological region of interest

$$\Omega_z = \left\{ (S, I_z, R, S_m, I_m) \in \mathbb{R}_+^5 : 0 \leq N_h \leq \frac{\Lambda}{\mu}; 0 \leq N_m \leq \frac{\Lambda_m}{\mu_m} \right\}. \tag{15}$$

It can also be shown that Ω_z is positively invariant under the flow of (14).

The DFE for the model (14) is given by

$$\mathbf{E}_{z_0} = \left(\frac{\Lambda}{\mu}, 0, 0, \frac{\Lambda_m}{\mu_m}, 0 \right). \tag{16}$$

Now, we will determine the basic reproduction number \mathcal{R}_z for the model (14). Similarly as in Sect. 2.1, the matrices \mathbf{F} , \mathbf{V} and \mathbf{FV}^{-1} are given by

$$\mathbf{F} = \begin{bmatrix} \beta_z \frac{\Lambda}{\mu} & \beta_m \frac{\Lambda}{\mu} \\ \alpha_m \frac{\Lambda_m}{\mu_m} & 0 \end{bmatrix}, \quad \mathbf{V} = \begin{bmatrix} \delta_z + \mu + \mu_z & 0 \\ 0 & \mu_m \end{bmatrix}, \quad \text{and} \quad \mathbf{FV}^{-1} = \begin{bmatrix} \frac{\beta_z}{\delta_z + \mu + \mu_z} & \frac{\beta_m}{\mu_m} \\ \frac{\alpha_m \Lambda_m \mu}{\Lambda \mu_m (\delta_z + \mu + \mu_z)} & 0 \end{bmatrix}.$$

Thus, the basic reproduction number for the model (14) is given by

$$\mathcal{R}_z = \rho(\mathbf{FV}^{-1}) = \mathcal{R}_{z_1} + \sqrt{(\mathcal{R}_{z_1})^2 + \bar{\mathcal{R}}_{z_2}} =: \mathcal{R}_{z_1} + \mathcal{R}_{z_2}, \tag{17}$$

where

$$\begin{aligned} \mathcal{R}_{z_1} &= \frac{\beta_z}{2(\mu_z + \delta_z + \mu)}, \quad \bar{\mathcal{R}}_{z_2} = \frac{\beta_m \alpha_m \Lambda_m \mu}{\Lambda \mu_m^2 (\mu_z + \delta_z + \mu)} \quad \text{and} \\ \mathcal{R}_{z_2} &= \sqrt{(\mathcal{R}_{z_1})^2 + \bar{\mathcal{R}}_{z_2}}. \end{aligned} \tag{18}$$

Remark 1 Note that if the transmission of ZIKV by sexual contact is not considered ($\beta_z = 0$), $\mathcal{R}_{z1} = 0$ and \mathcal{R}_z reduces to

$$\mathcal{R}_z|_{(\beta_z=0)} = \sqrt{\bar{\mathcal{R}}_{z2}} = \sqrt{\frac{\beta_m \alpha_m \Lambda_m \mu}{\Lambda \mu_m^2 (\mu_z + \delta_z + \mu)}}$$

indicating that sexual contact transmission of ZIKV has an impact on \mathcal{R}_z .

The following lemma makes it easier to determine the sign of \mathcal{R}_z .

Lemma 1 *Let us define*

$$\begin{aligned} \mathcal{R}_z^* &= 2\mathcal{R}_{z1} + \bar{\mathcal{R}}_{z2} \\ &= \mathcal{R}_z^2 + 2\mathcal{R}_{z1}(1 - \mathcal{R}_z). \end{aligned} \tag{19}$$

- i. If $\mathcal{R}_z^* < 1$, then $2\mathcal{R}_{z1} < 1$ and $\mathcal{R}_z < 1$.*
- ii. If $\mathcal{R}_z^* > 1$ and $2\mathcal{R}_{z1} < 1$, then $\mathcal{R}_z > 1$.*
- iii. If $\mathcal{R}_z^* > 1$ and $2\mathcal{R}_{z1} > 1$, then $\mathcal{R}_z < 1$.*
- iv. If $\mathcal{R}_z^* = 1$, then $\mathcal{R}_z = 1$.*

The proof of item *i.* can be found in Appendix A.1. Items *ii.* to *iv.* can be proved in a similar manner.

From the above lemma we can see that the sign of \mathcal{R}_z is determined by the signs of \mathcal{R}_z^* and $2\mathcal{R}_{z1}$.

Observe that the third equation in the system (14) has a unique equilibrium given by $R = \frac{\delta_z}{\mu} I_z$. Therefore, to determine the endemic equilibrium points of the system (14), we must solve the following system of algebraic equations:

$$\begin{cases} 0 = \Lambda - \left(\beta_m \mu \frac{I_m}{\mu S + (\mu + \delta_z) I_z} + \beta_z \mu \frac{I_z}{\mu S + (\mu + \delta_z) I_z} \right) S - \mu S \\ 0 = \left(\beta_m \mu \frac{I_m}{\mu S + (\mu + \delta_z) I_z} + \beta_z \mu \frac{I_z}{\mu S + (\mu + \delta_z) I_z} \right) S - (\mu + \mu_z + \delta_z) I_z \\ 0 = \Lambda_m - \alpha_m \mu \frac{I_z}{\mu S + (\mu + \delta_z) I_z} S_m - \mu_m S_m \\ 0 = \alpha_m \mu \frac{I_z}{\mu S + (\mu + \delta_z) I_z} S_m - \mu_m I_m. \end{cases} \tag{20}$$

Denoting S^* , S_m^* and I_m^* the coordinates of the endemic equilibrium solution, after some algebraic manipulations in (20), we found that:

$$S^* = \frac{\Lambda - (\mu + \mu_z + \delta_z) I_z^*}{\mu}, \quad S_m^* = \frac{\Lambda_m - \mu_m I_m^*}{\mu_m}, \quad I_m = \frac{\alpha_m \mu I_z^* S_m^*}{\mu_m [\mu S^* + (\mu + \delta_z) I_z^*]} \tag{21}$$

Replacing the above values into the first equation of (20), we get the following quadratic equations in the variable I_z :

$$aI_z^2 + bI_z + c = 0, \quad \text{where} \tag{22}$$

$$\begin{aligned}
 a &= \alpha_m \beta_z \mu^4 \mu_m \\
 b &= \Lambda \mu^4 \mu_m \alpha_m [\beta_z \mu_m + \beta_m \alpha_m \Lambda_m + (1 - 2\mathcal{R}_{z_1})] \\
 c &= \Lambda^2 \mu^2 \mu_m (1 - \mathcal{R}_z^*).
 \end{aligned}
 \tag{23}$$

Note that $a > 0$, and the signs of b and c depends on the sign of \mathcal{R}_z^* and $2\mathcal{R}_{z_1}$. We have the following possibilities.

- P1) If $\mathcal{R}_z^* < 1$, then $2\mathcal{R}_{z_1} < 1$ (Lemma 2.19 item *i*). Therefore $b > 0$, $c > 0$ and thus, the quadratic equation (22) has not any positive root.
- P2) If $\mathcal{R}_z^* > 1$, then $c < 0$ and regardless of the sign of b , the quadratic equation (22) has only one positive root given by

$$I_z^* = \frac{-b + \sqrt{b^2 - 4ac}}{2a}.
 \tag{24}$$

- P3) If $\mathcal{R}_z^* = 1$ and $2\mathcal{R}_{z_1} < 1$, then $c = 0$ and $b > 0$. Therefore, the quadratic equation (22) has as solution $I_z = -b/a$. Thus, there are no positive roots.
- P4) If $\mathcal{R}_z^* = 1$ and $b < 0$, the quadratic equation (22) has a positive root given by $I_z = -b/a$.

Remark 2 The case where $\mathcal{R}_z^* < 1$ and $2\mathcal{R}_{z_1} > 1$ (which results in $c > 0$ and $b < 0$, thus allowing for the existence of two positive roots of the quadratic equation (22) when $b^2 - 4ac > 0$) is not considered. According to Lemma 2.19, item *i.*, if $\mathcal{R}_z^* < 1$, then $2\mathcal{R}_{z_1} < 1$. Therefore, this scenario is inconsistent with the conditions of the lemma and is excluded from consideration.

Based on the information presented earlier, the quadratic equation (22) has only one positive root defined in (24) whenever $\mathcal{R}_z^* > 1$. The following proposition gives us the existence and stability conditions of the equilibrium points for the system (14).

Proposition 2 *The system (14) always has a DFE E_{z_0} defined in (16). If $\mathcal{R}_z^* > 1$ the system has an endemic equilibrium point given by*

$$E_z^* = (S^*, I_z^*, S_m^*, I_m^*),
 \tag{25}$$

with S^* , I_z^* , S_m^* and I_m^* defined in (21) and (24). Additionally, the following stability results hold:

- (i) If $\mathcal{R}_z^* < 1$, then E_{z_0} is GAS.
- (ii) If $\mathcal{R}_z^* > 1$, the endemic equilibrium point E_z^* is LAS in Ω_z defined in (15).

Proof (i) We will denote $\kappa = \mu_z + \delta_z + \mu$ and a reasoning analogous to that used in Proposition 1, with the functions:

$$V^*(S, I_z, R, S_m, I_m) = \left(S - \frac{\Lambda}{\mu} \log \frac{S\mu}{\Lambda} \right) + I_z + \frac{\beta_m \Lambda}{\mu \mu_m} \left(S_m - \frac{\Lambda_m}{\mu_m} \log \frac{S_m \mu_m}{\Lambda_m} \right) + \frac{\beta_m \Lambda}{\mu \mu_m} I_m$$

and

$$V(\bar{S}, \bar{I}_z, \bar{R}, \bar{S}_m, \bar{I}_m) = V^* \left(S - \frac{\Lambda}{\mu}, I_z, R, S_m, I_m - \frac{\Lambda_m}{\mu_m} \right).
 \tag{26}$$

We must prove that V defined in (26) is a Lyapunov function. V is positive definite and the orbital derivative of V along the trajectories of (14) is

$$\begin{aligned} \dot{V} &= \left(1 - \frac{\Lambda}{\mu S}\right) \dot{S} + \dot{I}_z + \frac{\beta_m \Lambda}{\mu \mu_m} \left(1 - \frac{\Lambda_m}{\mu_m S_m}\right) \dot{S}_m + \frac{\beta_m \Lambda}{\mu \mu_m} \dot{I}_m \\ &= \left(1 - \frac{\Lambda}{\mu S}\right) \left(\Lambda - \beta_m \frac{I_m}{N_z} S - \beta_z \frac{I_z}{N_z} S - \mu S\right) + \left(\beta_m \frac{I_m}{N_z} S + \beta_z \frac{I_z}{N_z} S - \kappa I_z\right) \\ &\quad + \frac{\beta_m \Lambda}{\mu \mu_m} \left(1 - \frac{\Lambda_m}{S_m \mu_m}\right) \left(\Lambda_m - \alpha_m \frac{I_z}{N_z} S_m - \mu_m S_m\right) + \frac{\beta_m \Lambda}{\mu \mu_m} \left(\alpha_m \frac{I_z}{N_z} S_m - \mu_m I_m\right) \\ &= (\Lambda - \mu S) - \frac{\Lambda}{\mu S} (\Lambda - \mu S) + \frac{\Lambda}{\mu S} \left(\beta_m \frac{I_m}{N_z} + \beta_z \frac{I_z}{N_z}\right) S - \kappa I_z + \frac{\beta_m \Lambda}{\mu \mu_m} (\Lambda_m - \mu_m S_m) \\ &\quad - \frac{\beta_m \Lambda \Lambda_m}{\mu \mu_m S_m \mu_m} (\Lambda_m - \mu_m S_m) + \frac{\beta_m \Lambda \Lambda_m \alpha_m S_m I_z}{\mu \mu_m S_m \mu_m} - \frac{\beta_m \Lambda \mu_m I_m}{\mu \mu_m} \\ &\leq -\frac{(\Lambda - \mu S)^2}{\mu S} - \frac{\beta_m \Lambda}{\mu \mu_m^2} \frac{(\Lambda_m - \mu_m S_m)^2}{S_m} + \left(\frac{\Lambda}{\mu} \beta_z + \frac{\beta_m \alpha_m \Lambda_m \Lambda}{\mu \mu_m^2} - \kappa\right) I_z \\ &= -\frac{(\Lambda - \mu S)^2}{\mu S} - \frac{\beta_m \Lambda}{\mu \mu_m^2} \frac{(\Lambda_m - \mu_m S_m)^2}{S_m} - \kappa (1 - \mathcal{R}_z^*) I_z. \end{aligned}$$

Note that the last expression in the above inequality is negative if $\mathcal{R}_z^* < 1$ and for $S = \frac{\Lambda}{\mu}$, $S_m = \frac{\Lambda_m}{\mu_m}$ and $I_z = I_m = 0$. Finally, using the LaSalle’s invariance principle (Hainzl et al. 2022), \mathbf{E}_{z_0} defined in (16) is a global attractor whenever $\mathcal{R}_z^* < 1$.

- (ii) We start by ordering equations and variables as S, S_m, I_z, I_m, R , and by making the following change of variables:

$$\begin{aligned} t_1 &= \frac{\beta_m I_m + \beta_z I_z}{N_z} \left(1 - \frac{S}{N_z}\right), \quad t_2 = \frac{\alpha_m S_m I_z}{N_z}, \quad t_3 = \frac{\alpha_m I_z}{N_z}, \\ t_4 &= \frac{\beta_m I_m + \beta_z I_z}{N_z^2} S, \quad t_5 = \frac{\beta_z S}{N_z}, \quad t_6 = \frac{\alpha_m S_m I_z}{N_z} \left(1 - \frac{I_z}{N_z}\right), \quad t_7 = \frac{\beta_m S}{N_z}. \end{aligned}$$

The Jacobian matrix of the system (14) at an arbitrary point $\mathbf{E} = (S, S_m, I_z, I_m, R)$, which is given by

$$\mathbf{J}(\mathbf{E}) = \begin{bmatrix} \mathbf{J}_{11}(\mathbf{E}) & \mathbf{0} \\ \star & -\mu, \end{bmatrix}. \tag{27}$$

Thus, the eigenvalues of $\mathbf{J}(\mathbf{E})$ are $-\mu < 0$ and those of $\mathbf{J}_{11}(\mathbf{E})$. Thus, the matrix $\mathbf{J}_{11}(\mathbf{E})$ at the endemic equilibrium \mathbf{E}_z^* in (25) can be written as:

$$\mathbf{J}_{11}(\mathbf{E}_z^*) = \begin{bmatrix} -(t_1 + \mu) & 0 & t_4 - t_5 & -t_7 \\ t_2 & -(\mu_m + t_3) & -t_6 & 0 \\ t_1 & 0 & -(\kappa + t_4) + t_5 & t_7 \\ -t_2 & t_3 & t_6 & -\mu_m \end{bmatrix}.$$

After some algebraic manipulations, we find that the characteristic polynomial associated with the matrix $\mathbf{J}(\mathbf{E}_z^*)$ is

$$r(y) = (y + \mu_m)(y^3 + b_1 y^2 + b_2 y + b_3), \quad \text{where}$$

$$b_1 = l_1 + \kappa(1 - 2\mathcal{R}_{z_1}), \quad b_2 = l_2 + \kappa(\mathcal{R}_z^* - 1), \quad b_3 = l_3(\mathcal{R}_z^* - 1), \quad (28)$$

and $l_i, i = 1, 2, 3$ are positive linear combinations of $t_i, i = 1, \dots, 7$. The characteristic polynomial $r(y)$ gives four roots $y = -\mu_m$, whereas the Routh-Hurwitz criteria assures that the other two roots have negative real part if $b_i > 0$ for $i = 1, 2, 3$ and $b_1b_2 - b_3 > 0$. Clearly the coefficients $b_i > 0, i = 1, 2, 3$ are all positive if $\mathcal{R}_z^* > 1$ and $1 - 2\mathcal{R}_{z_1} > 0$. Thus, it follows that the endemic equilibrium \mathbf{E}_z^* of the system (14) is LAS if $\mathcal{R}_z^* > 1$. □

3 Qualitative Behaviour of the HIV/ZIKV Model

In this section, we discuss the qualitative properties of the HIV/ZIKV co-infection model (2). To achieve this purpose, we use the existence and stability results as well as the definition of the basic reproduction number for the HIV model \mathcal{R}_h in (6) and \mathcal{R}_z in (17) obtained in Sects. 2.1 and 2.2.

In the model (2), the total human population is denoted by $N(t) = S(t) + I_z(t) + I_h(t) + I_{hz}(t) + A(t) + R(t)$, and the total mosquito population is $N_m(t) = S_m(t) + I_m(t)$. Additionally, to simplify algebraic calculations we rename parameters:

$$\begin{aligned} \kappa_1 &= \mu_z + \delta_z + \mu, & \kappa_2 &= \sigma_1 + \mu, \\ \kappa_3 &= \sigma_2 + \mu_{hz} + \mu, & \kappa_4 &= \mu_h + \mu. \end{aligned} \quad (29)$$

The interest region set is given by

$$\Omega = \left\{ (S, I_z, I_h, I_{hz}, A, R, S_m, I_m) \in \mathbb{R}_+^8 : 0 \leq N \leq \frac{\Lambda}{\mu}; 0 \leq N_m \leq \frac{\Lambda_m}{\mu_m} \right\}. \quad (30)$$

As in the previous sections, it can be proved that Ω is positively invariant under the flow of (2).

3.1 Computation of the Basic Reproduction Number

The DFE for the model (2) is given by

$$\mathbf{E}_0 = \left(\frac{\Lambda}{\mu}, 0, 0, 0, 0, 0, \frac{\Lambda_m}{\mu_m}, 0 \right). \quad (31)$$

Similarly to Sects. 2.1 and 2.2, the basic reproduction number associated to the model (2) can be determined through the matrices \mathbf{F} and \mathbf{V} given by

$$\mathbf{F} = \begin{bmatrix} \beta_z & 0 & \beta_z & 0 & \beta_m \\ 0 & \beta_h & \beta_h & 0 & 0 \\ 0 & 0 & \beta_z \beta_h & 0 & 0 \\ 0 & 0 & 0 & 0 & 0 \\ \frac{\alpha_m \Lambda_m \mu}{\Lambda \mu_m} & 0 & \frac{\alpha_m \Lambda_m \mu}{\Lambda \mu_m} & 0 & 0 \end{bmatrix},$$

$$\mathbf{V} = \begin{bmatrix} \kappa_1 & 0 & 0 & 0 & 0 \\ 0 & \kappa_2 & -\epsilon \delta_z & 0 & 0 \\ 0 & 0 & \epsilon \delta_z + \kappa_3 & 0 & 0 \\ 0 & -\sigma_1 & -\sigma_2 & \kappa_4 & 0 \\ 0 & 0 & 0 & 0 & \mu_m \end{bmatrix} \quad \text{and} \quad \mathbf{V}^{-1} = \begin{bmatrix} \frac{1}{\kappa_1} & 0 & 0 & 0 & 0 \\ 0 & \frac{1}{\kappa_2} & \frac{\epsilon \delta_z}{\kappa_2(\epsilon \delta_z + \kappa_3)} & 0 & 0 \\ 0 & 0 & \frac{1}{\epsilon \delta_z + \kappa_3} & 0 & 0 \\ 0 & \frac{\sigma_1}{\kappa_2 \kappa_4} & \frac{\epsilon \delta_z \sigma_1 + \kappa_2 \sigma_2}{\kappa_2 \kappa_4 (\epsilon \delta_z + \kappa_3)} & \frac{1}{\kappa_4} & 0 \\ 0 & 0 & 0 & 0 & \frac{1}{\mu_m} \end{bmatrix}.$$

Here, the matrix \mathbf{FV}^{-1} is given by

$$\mathbf{FV}^{-1} = \begin{bmatrix} \frac{\beta_z}{\kappa_1} & 0 & \frac{\beta_z}{\epsilon \delta_z + \kappa_3} & 0 & \frac{\beta_m}{\mu_m} \\ 0 & \frac{\beta_h}{\kappa_2} & \frac{\beta_h(\epsilon \delta_z + \kappa_3)}{\kappa_2(\epsilon \delta_z + \kappa_3)} & 0 & 0 \\ 0 & 0 & \frac{\beta_z \beta_h}{\epsilon \delta_z + \kappa_3} & 0 & 0 \\ 0 & 0 & 0 & 0 & 0 \\ \frac{\alpha_m \Lambda_m \mu}{\kappa_1 \Lambda \mu_m} & 0 & \frac{\alpha_m \Lambda_m \mu}{\Lambda(\epsilon \delta_z + \kappa_3) \mu_m} & 0 & 0 \end{bmatrix}.$$

The above matrix has as eigenvalues: $\lambda_1 = 0$, $\lambda_2 = \frac{\beta_z \beta_h}{\epsilon \delta_z + \kappa_3} = \frac{\beta_z \beta_h}{\epsilon \delta_z + \sigma_2 + \mu_{hz} + \mu}$, and $\lambda_3 = \frac{\beta_h}{\kappa_2} = \mathcal{R}_h$, whereas the other two eigenvalues are

$$\lambda_{4,5} = \frac{\beta_z}{2\kappa_1} \pm \sqrt{\left(\frac{\beta_z}{2\kappa_1}\right)^2 + \frac{\alpha_m \beta_m \Lambda_m \mu}{\Lambda \mu_m^2 \kappa_1}} = \mathcal{R}_{z1} \pm \mathcal{R}_{z2},$$

with the positive eigenvalues being

$$\lambda_4 = \frac{\beta_z}{2\kappa_1} + \sqrt{\left(\frac{\beta_z}{2\kappa_1}\right)^2 + \frac{\alpha_m \beta_m \Lambda_m \mu}{\Lambda \mu_m^2 \kappa_1}} = \mathcal{R}_{z1} + \mathcal{R}_{z2} = \mathcal{R}_z.$$

Thus, the basic reproduction number for the model (2) is given by

$$\mathcal{R}_0 = \rho(\mathbf{FV}^{-1}) = \max\{\mathcal{R}_h, \mathcal{R}_z^*, \mathcal{R}_{hz}\}, \tag{32}$$

where

$$\mathcal{R}_{hz} := \frac{\beta_z \beta_h}{\epsilon \delta_z + \sigma_2 + \mu_{hz} + \mu}, \tag{33}$$

\mathcal{R}_h is the basic reproduction number for the HIV model defined in the equation (6) and $\mathcal{R}_z = \mathcal{R}_{z_1} + \mathcal{R}_{z_2}$ is the basic reproduction number of the ZIKV model, which is defined in the equation (17). From the calculation of \mathcal{R}_0 , the local asymptotic stability of the DFE follows.

Proposition 3 *If $\mathcal{R}_0 = \max\{\mathcal{R}_h, \mathcal{R}_z, \mathcal{R}_{hz}\} < 1$, then E_0 defined in (31) is LAS in Ω defined in (30).*

Techniques similar to those used in Sects. 2.1 and 2.2 can be applied to confirm the presence of endemic solutions and assess their local and global stability.

3.2 Local Sensitivity Analysis of the Parameters

The local sensitivity analysis of \mathcal{R}_0 with respect to the model parameters allows quantifying parameter variations' effect on the value of \mathcal{R}_0 . The sign of the sensitivity index denotes the direction of the change, where a positive index for a particular parameter indicates that increasing that parameter will increase \mathcal{R}_0 and vice-versa. In addition, the sensitivity index's magnitude provides insight into each parameter's impact on the predictions (Saltelli et al. 2008).

The normalized sensitivity index of a variable concerning a parameter is a measure of how much the variable relatively changes to the change in the parameter (Chitnis et al. 2008) and is defined as:

$$\Gamma_p^X = \frac{\partial X}{\partial p} \frac{p}{X}. \quad (34)$$

Because \mathcal{R}_0 is defined as $\max\{\mathcal{R}_h, \mathcal{R}_z, \mathcal{R}_{hz}\}$, the sensitivity indices of \mathcal{R}_0 with respect to the eleven parameters $\{\beta_h, \Lambda, \mu, \sigma_1, \beta_z, \mu_z, \delta_z, \beta_m, \alpha_m, \Lambda_m, \mu_m, \epsilon, \mu_{hz}\}$ in the expression of \mathcal{R}_0 in (32), can be determined for the sensitivity indices of \mathcal{R}_h , \mathcal{R}_z and \mathcal{R}_{hz} , respectively. A calculation example of the sensitivity index of \mathcal{R}_z with respect to the parameter β_z can be found in Appendix A.2.

4 The Control Problem Analysis

In this section, we present an optimal control problem (OCP) by including three interventions to manage how HIV/ZIKV co-infection spreads within our model (2). The proposed approach mitigates HIV and Zika infections by implementing personal protection measures (such as the use of repellents) using control η_1 , ART with control η_2 , and preventive sexual contact (such as the use of condoms) with control η_3 (see Table 1). The control functions η_1 , η_2 and η_3 are defined in the interval $[0, T]$, where T denotes the final time of the controls, $0 \leq \eta_i(t) \leq 1$ and $t \in [0, T]$ for $i = 1, 2, 3$. Furthermore, depending on the nature of the problem, different types of cost function may be appropriate. In general, the forms used in the cost function depend on the specific context and characteristics of the problem, allowing a balance in terms of the benefits of disease control and the costs associated with interventions. For example, an exponential cost function, due to its concave nature, is suitable in situations of high uncertainty because it reflects a greater concern for unfavorable events (see, e.g.,

Avusuglo et al. 2023; Grandits et al. 2019). Conversely, a quadratic cost function, due to its convex nature, is useful when seeking to ensure that the solutions found are globally optimal, which simplifies the optimization process and is particularly valuable in problems where precision and certainty are crucial (see, e.g., Romero-Leiton et al. 2019). Therefore, the following OCP is formulated by a hybrid cost function combining linear and quadratic terms, where the controls are shown in red for emphasis.

$$\left\{ \begin{array}{l}
 \min \mathcal{J}(\eta) = \int_0^T \left(c_1 I_z + c_2 I_h + c_3 I_{hz} + c_4 I_m + c_5 A + d_1 \frac{\eta_1^2}{2} + d_2 \frac{\eta_2^2}{2} + d_3 \frac{\eta_3^2}{2} \right) dt \\
 \frac{dS}{dt} = \Lambda - (1 - \eta_1)\tilde{\beta}_m S - (1 - \eta_3)(\tilde{\beta}_c + \tilde{\beta}_z + \tilde{\beta}_h)S - \mu S \\
 \frac{dI_z}{dt} = (1 - \eta_1)\tilde{\beta}_m S + (1 - \eta_3)\tilde{\beta}_z S - \omega_2(1 - \eta_3)\tilde{\beta}_h I_z - (\mu_z + \delta_z + \mu)I_z \\
 \frac{dI_h}{dt} = \epsilon \delta_z I_{hz} + (1 - \eta_3)\tilde{\beta}_h S - \omega_1[(1 - \eta_1)\tilde{\beta}_m + (1 - \eta_3)\tilde{\beta}_z]I_h - (1 - \eta_2)\sigma_1 I_h - \mu I_h \\
 \frac{dI_{hz}}{dt} = (1 - \eta_3)\tilde{\beta}_c S + \omega_2(1 - \eta_3)\tilde{\beta}_h I_z + \omega_1[(1 - \eta_3)\tilde{\beta}_z + (1 - \eta_1)\tilde{\beta}_m]I_h \\
 \quad - \epsilon \delta_z I_{hz} - (1 - \eta_2)\sigma_2 I_{hz} - (\mu_{hz} + \mu)I_{hz} \\
 \frac{dA}{dt} = (1 - \eta_2)\sigma_1 I_h + (1 - \eta_2)\sigma_2 I_{hz} - (\mu_h + \mu)A \\
 \frac{dR}{dt} = \delta_z I_z - \mu R \\
 \frac{dS_m}{dt} = \Lambda_m - (1 - \eta_1)\tilde{\alpha}_m S_m - \mu_m S_m \\
 \frac{dI_m}{dt} = (1 - \eta_1)\tilde{\alpha}_m S_m - \mu_m I_m \\
 \mathbf{X}(0) = (S_0, I_{z0}, I_{h0}, I_{hz0}, A_0, R_0, S_{m0}, I_{m0}) = \mathbf{X}_0 \\
 \mathbf{X}(T) = (S_f, I_{zf}, I_{hf}, I_{hzf}, A_f, R_f, S_{mf}, I_{mf}) = \mathbf{X}_f.
 \end{array} \right. \tag{35}$$

In the above formulation $\eta = (\eta_1(t), \eta_2(t), \eta_3(t))$, and $c_1, c_2, c_3, c_4, c_5, d_1, d_2$, and d_3 are positive weights. Therefore, we seek an optimal control $\eta^*(t)$ determined as

$$\mathcal{J}(\eta^*(t)) = \min \{ \mathcal{J}(\eta(t) | \eta \in \mathcal{A}) \}, \tag{36}$$

with a set \mathcal{A} of controls defined as

$$\mathcal{A} = \{ \eta(t) = (\eta_1(t), \eta_2(t), \eta_3(t)) | 0 \leq \eta_1(t) \leq \eta_1^{\max}, 0 \leq \eta_2(t) \leq \eta_2^{\max}, 0 \leq \eta_3(t) \leq \eta_3^{\max} \},$$

where $\eta_i^{\max} \leq 1, i = \{1, 2, 3\}$ and η is Lebesgue measurable. In order to define the formulation of our OCP using Pontryagin’s Maximum Principle (PMP) (Pontryagin et al. 2018), we have the Lagrangian as

$$L = c_1 I_z(t) + c_2 I_h(t) + c_3 I_{hz}(t) + c_4 I_m(t) + c_5 A(t) + d_1 \frac{\eta_1^2(t)}{2} + d_2 \frac{\eta_2^2(t)}{2} + d_3 \frac{\eta_3^2(t)}{2}, \tag{37}$$

and we determine the Hamiltonian function as

$$H = L(I_z, I_h, I_{hz}, I_m, A, \eta) + p_1 \frac{dS}{dt} + p_2 \frac{dI_z}{dt} + p_3 \frac{dI_h}{dt} + p_4 \frac{dI_{hz}}{dt} + p_5 \frac{dA}{dt}$$

$$+ p_6 \frac{dR}{dt} + p_7 \frac{dS_m}{dt} + p_8 \frac{dI_m}{dt}. \tag{38}$$

In the remainder, we investigate the minimum value of Lagrangian (37). Firstly, we must prove the existence of the optimal control η^* according to the controlled system (35).

Proposition 4 *There exists an optimal control η^* such that*

$$\mathcal{J}(\eta^*(t)) = \min_{\eta \in \mathcal{A}}(\mathcal{J}(\eta(t))),$$

subject to the control system (35) with initial conditions as \mathbf{X}_0 .

The proof of the above proposition can be found in Appendix A.3.

In the following, we apply PMP (Pontryagin et al. 2018) to provide a characterization of an optimal control solution to the Hamiltonian (38) subject to the OCP (35). If (X^*, η^*) is an optimal solution for the controlled system (35), then there exists a non trivial vector function $p = (p_1, p_2, p_3, p_4, p_5, p_6, p_7, p_8)$, such that

$$\frac{\partial H}{\partial \eta_i} = 0, \quad i = 1, 2, 3 \quad \text{and} \quad \dot{p}_i = \frac{dp_i}{dt} = -\frac{\partial H}{\partial X_i}, \quad i = 1, \dots, 8. \tag{39}$$

Proposition 5 *Let $(S^*, I_z^*, I_h^*, I_{hz}^*, A^*, R^*, S_m^*, I_m^*)$ be the optimal state variables solution associated to the optimal control variable η^* subject to the control problem (36). Then, there exists an adjoint vector p that satisfies the controlled system (35), with transversality conditions $p_i(T) = 0$, for $i = 1, \dots, 8$, where the optimal controls are*

$$\begin{aligned} \eta_1^* &= \frac{(p_2 - p_1)\tilde{\beta}_m S + (p_4 - p_3)\omega_1 \tilde{\beta}_m I_h + (p_8 - p_7)\tilde{\alpha}_m S_m}{d_1} \\ \eta_2^* &= \frac{(p_5 - p_3)\sigma_1 I_h + (p_5 - p_4)\sigma_2 I_{hz}}{d_2} \\ \eta_3^* &= \frac{(p_2 - p_1)\tilde{\beta}_z S + (p_3 - p_1)\tilde{\beta}_h S + (p_4 - p_1)\tilde{\beta}_c S + (p_4 - p_3)\omega_1 \tilde{\beta}_z I_h + (p_4 - p_2)\omega_2 \tilde{\beta}_h I_z}{d_3}. \end{aligned} \tag{40}$$

The proof is in Appendix A.4.

5 HIV/ZIKV Co-infection in Brazil and Colombia

As said before, in 2015, there was a concerning event in Brazil and Colombia associated with the co-infection of Zika and HIV/AIDS (Calvet et al. 2016; Brasil et al. 2016; Smith and Mackenzie 2016). Due to the absence of temporal records on HIV/ZIKV co-infection to date, it was not possible to estimate the parameters of the model (2) in this section. However, the values of specific parameters were derived from available

demographic information, previous research on Zika and HIV/AIDS in Colombia and Brazil, and epidemiological assumptions. When there were insufficient data available, these values were estimated based on specific assumptions or adapted from research conducted in different regions or diseases. The following outlines the main assumptions for extracting these parameter values: (1) The precise ratio between humans infected population and population densities of *Aedes aegypti* is difficult to assess. In fact, the entomological and biological characteristics of these mosquitoes, including their population size and geographical location or distribution, are impacted by meteorological factors, including but not limited to temperature and precipitation (Heinisch et al. 2019). Therefore, to facilitate our numerical experiments and to not lose generality, we assume that during 2015, there existed an approximate ratio of one human to three female *Aedes aegypti* mosquitoes (1:3) in Colombia and Brazil; (2) The scale parameter ϵ , which modifies the mean duration of Zika infection $1/\delta_z$ in co-infected individuals, was estimated to range from 0.77–0.88. This suggests that if the mean duration of Zika infection typically ranges between 8 and 15 days, in a co-infected individual, this interval could vary by approximately two days. This estimate is based on research showing that people co-infected with HIV/ZIKV tend to recover more slowly than those infected only with Zika (Rothan et al. 2018; Aschengrau et al. 2021; Bidokhti et al. 2018). In fact, a previous study on HIV-infected pregnant women in Brazil (Hainzl et al. 2022) revealed that although the overall proportion of Zika infections was approximately 5%, the rate of neurological complications in newborns was significantly higher. This rate reached 12% among those co-infected with both viruses, suggesting that a lower scale parameter value is associated with a higher likelihood of neurological problems in the infants of co-infected women; (3) In 2015, only a few cases were reported in Colombia and Brazil (Calvet et al. 2016; Smith and Mackenzie 2016), leading us to assume that the parameters related to the co-infection probability, ω_1 and ω_2 , were sufficiently small. Furthermore, we assumed that the probability that an HIV-infected individual contracting Zika is higher than that of a Zika-infected individual contracting HIV. This assumption is based on the fact that the immune system of an HIV-infected person is generally weaker than that of a ZIKV-infected person (Rothan et al. 2018). To explore the impact of varying co-infection probabilities, we also present a hypothetical scenario in which these parameters are increased, illustrating the correlation between higher co-infection probabilities and the resultant increase in the number of co-infected individuals; (4) According to demographic statistics for 2015, Colombia had approximately a population size of 47,630,000 inhabitants, while for Brazil was 206,900,000. It was assumed that 0.8% of the population in both countries had Zika infection, with 0.6% effectively recovered. In addition, 0.4% of the population had HIV and 0.3% progressed to AIDS due to untreated conditions. It was assumed that 0.01% of the population contracted co-infection with both diseases. For mosquitoes population, we assumed that for 2015, 15% were ZIKV-carrier. Finally, some parameter values on HIV/AIDS were conveniently adjusted at the population level, using estimates obtained from Luxembourg, the Czech Republic, Japan, Croatia, the United Kingdom and Mexico (Prieto and Romero-Leiton 2021). Finally, we suppose that Colombia and Brazil share some common parameter values (see Table 3), particularly excluding those related to the magnitude of the nation's population and its initial conditions (see Tables 4 and 5). Due to the dispersion of the units of measure-

Table 3 Shared (Colombia-Brazil) range of parameter values (minimum and maximum) involved in the model (2). Time in days

Parameter	Symbol	Range	Reference
Mean duration of Zika infection	$1/\delta_z$	[8, 15]	[XXX]
Mean duration of the HIV-immunodeficiency period	$1/\sigma_1$	[8, 10]	(Prieto and Romero-Leiton 2021)
Human mean lifespan	μ	[2.70e4, 2.78e4]	[XXX]
Mortality rate by AIDS	μ_h	0.002	(Prieto and Romero-Leiton 2021)
Mosquito mean lifespan	$1/\mu_m$	[14, 50]	(Gao et al. 2016)
Mortality rate by Zika	μ_z	[9e-5, 1.4e-4]	Assumed
Mortality rate by ZIKV/AIDS	μ_{hz}	0	(Calvet et al. 2016; Smith and Mackenzie 2016)
Mean duration of the HIV immunodeficiency period in co-infected individuals	$1/\sigma_2$	[6, 8]	(Calvet et al. 2016; Smith and Mackenzie 2016)
Transition probability from HIV to HIV/ZIKV co-infection	ω_1	0.045	Assumed
Transition probability from ZIKV to HIV/ZIKV co-infection	ω_2	0.005	Assumed
Scaling factor for Zika recovery in co-infected individuals	ϵ	[0.77, 0.88]	Assumed

Table 4 Range of parameter values (minimum and maximum) involved in the model (2) that differ in Colombia and Brazil. Time in days

Parameter	Symbol	Colombia	Brazil	Reference
ZIKV infection rate of humans by mosquitoes	β_m	[0.003, 0.01]	[0.005, 0.02]	(Gao et al. 2016)
ZIKV infection rate by sexual contact	β_z	[2e-3, 1.25e-3]	[6e-4, 2.1e-3]	(Gao et al. 2016)
HIV infection rate by sexual contact	β_h	[3e-4, 7e-4]	[3.2e-4, 7.9e-4]	(Prieto and Romero-Leiton 2021)
HIV/ZIKV co-infection rate by sexual contact	β_c	[6e-7, 8.75e-7]	[2.5e-6, 3.4e-7]	Assumed
ZIKV infection rate of mosquitoes by humans	α_m	[0.03, 0.1]	[0.07, 0.12]	(Gao et al. 2016)
Recruitment of humans	Λ	1,738.49	7,551.85	Computed
Recruitment of mosquitoes	Λ_m	7,644.615	33,207.450	Computed

Table 5 Initial conditions involved in the model (2), which correspond to the population sizes in Colombia [35] and Brazil [36] in 2015. Colombia—47,630,000 inhabitants; Brazil—206,900,000 inhabitants. Zika infection percentage: 0.8%, Zika recovery percentage: 0.6%, HIV infection percentage: 0.4%, AIDS progression percentage: 0.3%, Co-infection percentage: 0.01%. Mosquitoes ZIKV-carrier percentage: 15%

Parameter	Colombia	Brazil	Reference
$S(0)$	46,625,007	202,534,410	(Castillo-Chavez and Thieme 1994; Brasil et al. 2016)
$I_z(0)$	381,040	1,655,200	Computed
$I_h(0)$	190,520	827,600	Computed
$I_{hz}(0)$	4,763	20,690	(Calvet et al. 2016; Smith and Mackenzie 2016)
$A(0)$	142,890	620,700	Computed
$R(0)$	285,780	1,241,400	Computed
$S_m(0)$	121,456,500	527,595,000	Computed
$I_m(0)$	21,433,500	93,105,000	Computed

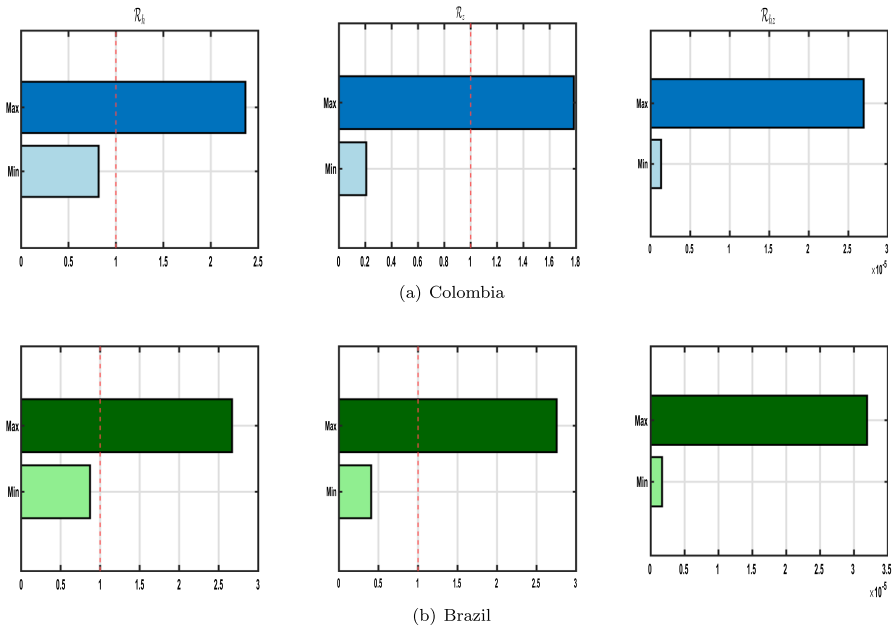


Fig. 2 Possible values for the thresholds using the extreme parameter values given in Tables 3 and 4 for Colombia (blue bars) and Brazil (green bars). In each case, $\mathcal{R}_0 = \max\{\mathcal{R}_h, \mathcal{R}_z, \mathcal{R}_{hz}\}$. The vertical red line represents $\mathcal{R}_{h,z,hz} = 1$ (Color figure online)

ment of the parameters in the different sources consulted, all parameter values were adapted to *day* as the standard unit of measurement.

Therefore, our case study is organized into three separate stages: (1) In the initial stage, we seek to numerically determine the basic reproduction number associated with the co-infection epidemic model (2), and we determine the numerical values of the sensitivity indices determined analytically in Sect. 3.2. (2) Next, we numerically simulate the uncontrolled model defined by (2). We then compare the incidence of infectious compartments in a range of parameter values for different scenarios of \mathcal{R}_0 . (3) In this stage, we explore hypothetical scenarios for the co-infected compartment by varying the parameters ϵ , δ_z , ω_1 , and ω_2 . (4) Finally, we focus on numerically simulating the control problem described in (35).

5.1 The Basic Reproduction Number and its Sensitivity Indices

In Sect. 3.1, we calculated the basic reproduction number (32) for the model (2). Figure 2 shows the possible values for the basic reproduction number using the values of extreme parameters given in Tables 3 and 4 for Colombia and Brazil, which result in the minimum or maximum value of \mathcal{R}_0 , respectively. Figure 2 shows that Brazil has the highest basic reproduction numbers compared to Colombia, which could be due to Brazil’s much larger population. In both countries, the basic reproduction number for individuals infected only with HIV is higher than for those infected only with

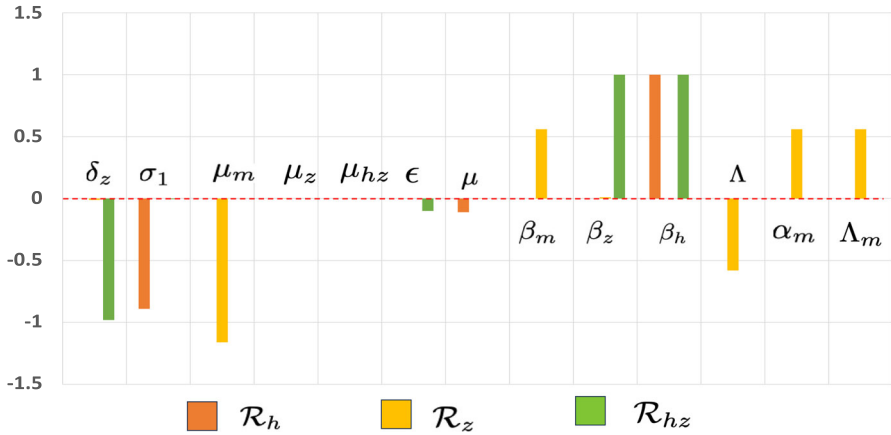


Fig. 3 Normalized sensitivity index of \mathcal{R}_h to the parameters $\{\beta_h, \mu, \sigma_1\}$, \mathcal{R}_z to the parameters $\{\Lambda, \mu, \beta_z, \mu_z, \delta_z, \beta_m, \alpha_m, \Lambda_m, \mu_m\}$ and \mathcal{R}_{hz} to the parameters $\{\beta_h, \beta_z, \delta_z, \epsilon, \mu_{hz}, \sigma_2, \mu\}$. Thus, the red dot line represents a sensitivity of zero. An example of calculation using Equation (34) can be found in Appendix A.2 (Color figure online)

ZIKV. Additionally, the basic reproduction number for only co-infected individuals is the lowest, which aligns with the small number of co-infection cases reported in both countries in 2015.

The normalized sensitivity indices of \mathcal{R}_h , \mathcal{R}_z and \mathcal{R}_{hz} are summarized in Fig. 3 and obtained using the values of the parameters in Tables 3 and 4.

For \mathcal{R}_h , the most significant parameters are the probability of HIV transmission through sexual contact β_h , followed by the average duration of the immunodeficiency period $1/\sigma_1$. For \mathcal{R}_z , the results indicate that the most important parameter is the mosquito death rate μ_m . In contrast, for \mathcal{R}_{hz} , the most critical parameters are the rates of Zika and HIV transmission through sexual contact β_z and β_h , and the average duration of Zika infection $1/\delta_z$. These results suggest that when developing strategies to combat HIV, Zika and co-infection, efforts should focus on parameters that reduce the risk of sexual transmission, such as the use of condoms, increasing mosquito mortality rates through insecticides, strengthening personal protection to avoid mosquito bites, improving Zika cure rates and reducing the transition to AIDS through antiretroviral therapy (ART).

5.2 Evaluation of Uncontrolled Population Behaviour Over Time

We numerically simulate the uncontrolled model defined by (2) by comparing the behaviour of the infectious compartments for different scenarios of \mathcal{R}_0 . From Fig. 4, we observed a trend of increasing numbers of infectious individuals (those infected only with Zika, only with HIV, co-infected, and ZIKV-carrying mosquitoes) with the increase in the basic reproduction number \mathcal{R}_0 in Colombia and Brazil during the first year (approximately 360 days). However, after the first year and up to approximately two years (2017) from the initial observation (2015), the behaviour of the number of

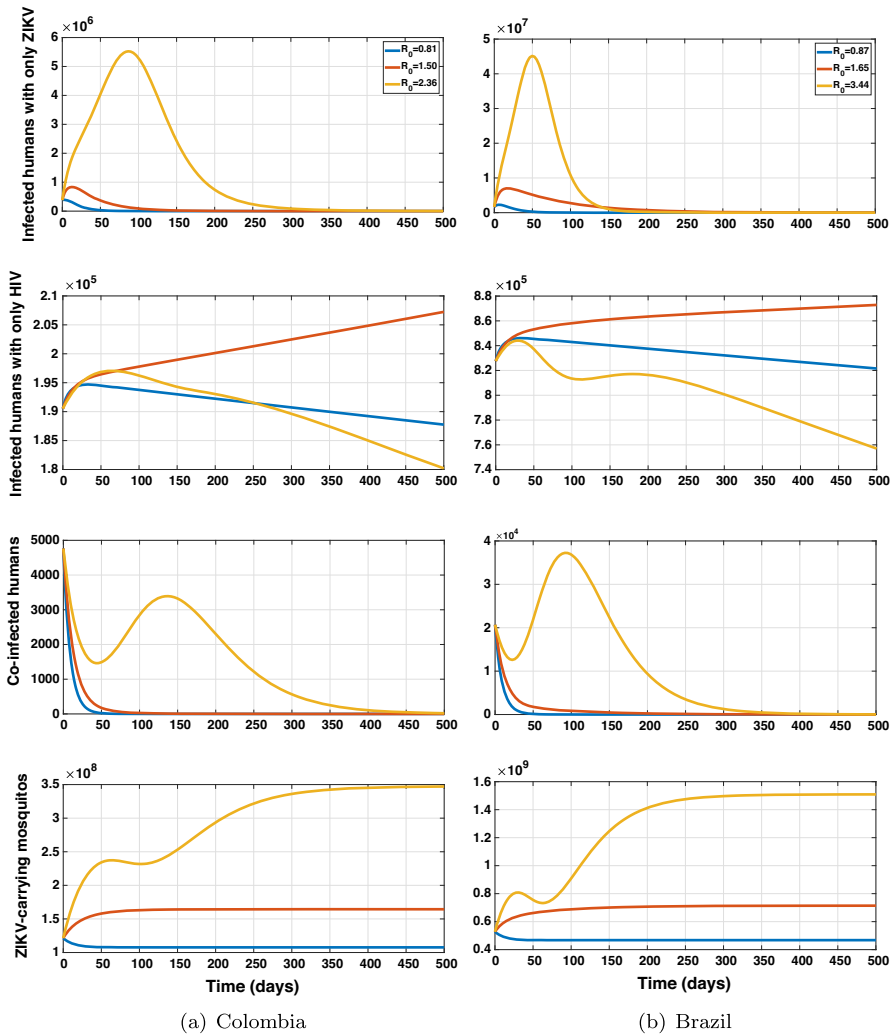


Fig. 4 Simulations of the infectious compartments for different values of \mathcal{R}_0 . We used the parameter values from Tables 4 and 5 that produce the minimum, medium and maximum basic reproduction numbers. For Colombia, the minimum values are $\mathcal{R}_h = 0.81$, $\mathcal{R}_z = 0.15$, and $\mathcal{R}_{hz} = 1.29 \times 10^{-6}$; the intermediate values are $\mathcal{R}_h = 1.50$, $\mathcal{R}_z = 0.57$, and $\mathcal{R}_{hz} = 7.65 \times 10^{-6}$; and the maximum values are $\mathcal{R}_h = 2.35$, $\mathcal{R}_z = 2.23$, and $\mathcal{R}_{hz} = 2.69 \times 10^{-5}$. For Brazil, the minimum values are $\mathcal{R}_h = 0.87$, $\mathcal{R}_z = 0.29$, and $\mathcal{R}_{hz} = 1.65 \times 10^{-6}$; the average values are $\mathcal{R}_h = 1.65$, $\mathcal{R}_z = 0.95$, and $\mathcal{R}_{hz} = 9.08 \times 10^{-6}$; and the maximum values are $\mathcal{R}_h = 2.67$, $\mathcal{R}_z = 3.44$, and $\mathcal{R}_{hz} = 3.19 \times 10^{-5}$ (Color figure online)

infectious individuals changed. For instance, the number of individuals infected only with Zika tends to decrease, regardless of the value of the basic reproduction number, and shows a peak during the first 30-150 days, reaching approximately 6 million infections in Colombia by day 60 and 50 million in Brazil by day 50. In the case of people infected solely with HIV, higher \mathcal{R}_0 values lead to a greater burden of HIV-only infections in both countries; however, this is only true for \mathcal{R}_0 values less than two; for

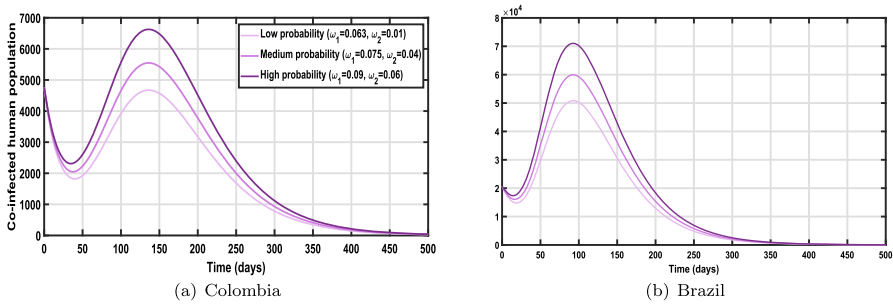


Fig. 5 Hypothetical scenario of ZIKV/HIV co-infection for different values of the co-infection probabilities ω_1 and ω_2 (high, medium, and low). The initial conditions are in Table 5 (population sizes in 2015) and the set of values of the parameters for the maximum vale of \mathcal{R}_0 (Color figure online)

higher values, the number of people infected solely with HIV decreases, perhaps due to the influence of people infected with Zika or co-infected. People who were co-infected had a profile similar to that of people infected with Zika alone, but to a lesser extent; in Colombia, the number of co-infected people fell after day 150, and in Brazil, after day 100. Additionally, a peak was also observed during these days, reaching approximately 3,200 co-infected individuals in Colombia by day 140 and 39,000 in Brazil by day 90. It is important to note that Zika-carrying mosquitoes exhibited similar behaviour across the three \mathcal{R}_0 values used as examples in our simulations, although their density increased by more than 10% in each case. These results are consistent, as no control measures were applied to the mosquito population.

These results can be explained by the fact that \mathcal{R}_0 represented in each case the maximum value among the basic reproduction numbers for Zika, HIV and co-infected individuals. In all three scenarios, \mathcal{R}_h was the highest, indicating that primary control efforts should focus on reducing sexual transmission. For large values of \mathcal{R}_0 , the populations of individuals infected only with Zika and co-infected individuals showed peaks, unlike those infected only with HIV. This indicates that Zika outbreaks occur only in certain seasons, whereas HIV cases remain constant over time.

In the actual context of co-infection cases in Colombia and Brazil, the probabilities of co-infection ω_1 and ω_2 were low, and the mean duration of Zika infection $1/\delta_z$ as well as the scaling factor for Zika cure ϵ were fixed. We therefore consider three hypothetical scenarios for people co-infected with HIV and ZIKV, as shown in Figs. 5, 6 and 7. In these cases, we used the initial conditions described in Table 5 (population sizes in 2015) and the set of parameter values for the maximum value of \mathcal{R}_0 .

In Fig. 5, we contrast three different possibilities for the probability of co-infection: Low probability ($\omega_1=0.063, \omega_2=0.01$), medium probability ($\omega_1=0.075, \omega_2=0.04$) and high probability ($\omega_1=0.09, \omega_2=0.06$). We can see that for higher values of this pair of parameters, the size of the population of individuals co-infected with ZIKV and HIV is larger. Clearly, an increase in these two probabilities increases the number of co-infected individuals.

Figure 6 shows the behaviour of co-infected individuals for different values of the mean duration of Zika virus infection $1/\delta_z$ and the scaling factor on Zika virus cure in co-infected individuals ϵ . It is generally estimated that a person recovers from Zika

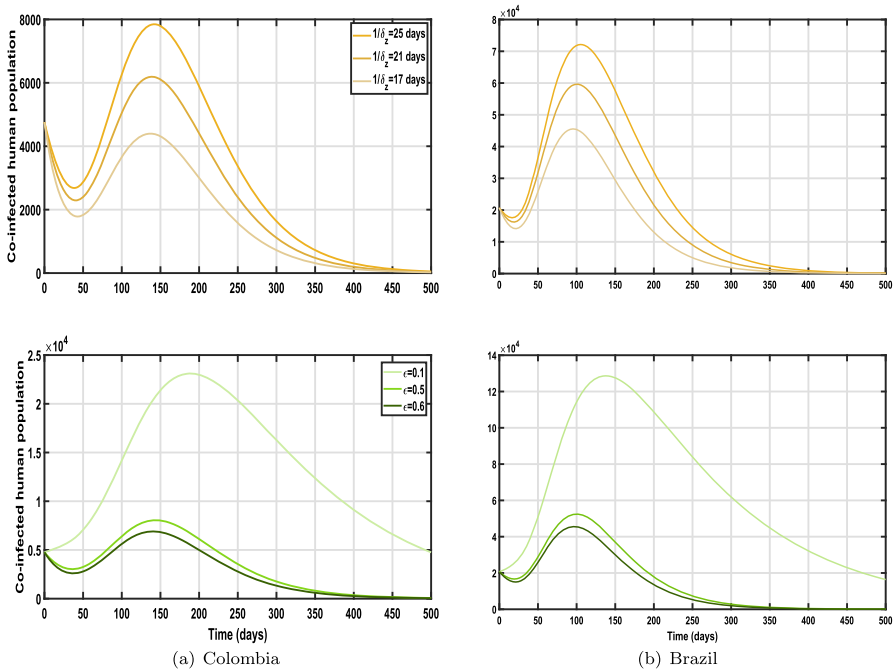


Fig. 6 Simulations of the system (2) for different values of the parameters δ_z and ϵ , using the parameter values from Tables 3 and 4, where \mathcal{R}_0 reaches its maximum value and the co-infection probabilities are $\omega_1 = 0.09$ and $\omega_2 = 0.06$. For variations in δ_z , $\epsilon = 0.77$ is fixed; for variations in ϵ , $1/\delta_z = 15$ is fixed (Color figure online)

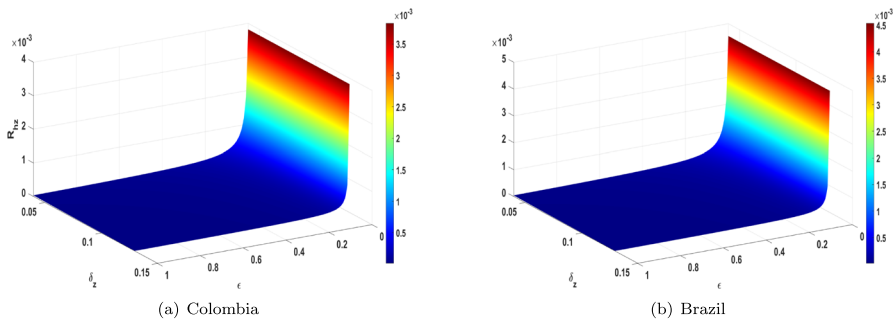


Fig. 7 Simulations of the basic reproduction number associated to co-infected individuals \mathcal{R}_{hz} for different values of ϵ and δ_z using the parameter values from Tables 3 and 4, where \mathcal{R}_0 reaches its maximum value and the co-infection probabilities are $\omega_1 = 0.09$ and $\omega_2 = 0.06$ (Color figure online)

within 8 to 15 days of the onset of symptoms (Patterson et al. 2016). However, for people infected with HIV, recovery time can be prolonged. We then considered a scenario in which the recovery times were 17, 21, and 25 days, keeping the parameter ϵ fixed at 0.77. We observed that, as the mean duration of Zika increased, the burden of co-infected individuals also increased. In fact, the more a person is infected with the Zika virus, the greater the risk of contracting HIV. The graphs showing the variations in

ϵ reinforce these findings. Indeed, by varying the parameter ϵ to 0.1, 0.5, and 0.6, while keeping the parameter $1/\delta_z$ fixed at 15 days, we observed that the lower the scaling parameter, the greater the number of co-infected individuals. In other words, increasing the recovery rate from Zika in co-infected individuals results in a higher number of co-infected individuals in the population. Although the parameters ϵ and δ_z did not have a significant impact on \mathcal{R}_0 in our results because their importance lied primarily in \mathcal{R}_{hz} , this hypothetical scenario suggests that varying these parameters in different contexts could make them highly influential when studying the dynamics of Zika and HIV co-infection. Therefore, in Fig. 7, we observe how the basic reproduction number associated with co-infected individuals \mathcal{R}_{hz} varies as the parameters $0 < \epsilon < 1$ and $8 < 1/\delta_z < 25$ ($0.04 < \delta_z < 0.13$) remain within its real range, resulting in values of $0 < \mathcal{R}_{hz} < 0.0004$ for Colombia and $0 < \mathcal{R}_{hz} < 0.00045$ in Brazil. It is clear that lower values of both parameters lead to a considerable increase in \mathcal{R}_{hz} , with a particularly rapid increase when $\epsilon < 0.2$. Therefore, we can conclude that the critical values $\epsilon < 0.2$ increase considerably \mathcal{R}_{hz} , which means that when the duration of Zika virus infection in co-infected people $1/\epsilon\delta_z > 40$ days, there could be a sharp increase in the number of co-infected people.

5.3 Evaluation of Controlled Population Behaviour Over Time

To reduce the spread of ZIKV and HIV in Colombia, targeted intervention strategies were implemented. In fact, this was a priority for the Colombian government's Zika strategic plan in 2016, when several measures were taken to improve surveillance and mitigate the burden of disease ([37], Forero-Martínez et al. 2020) such as health campaigns and funding for insecticides, larvicides and mosquito nets. In addition, to ensure that people living with HIV in Colombia receive the care they need to stay healthy and to reduce the risk of transmitting the virus to others, it was imperative to improve access to laboratory tests and HIV treatment (Galindo-Quintero et al. 2014). The use of condoms and other methods of reducing infection should also be encouraged as part of public health campaigns, particularly among high-risk groups. (Donoghoe et al. 2006). Brazil has also implemented a nationwide strategy to manage *Aedes* mosquito populations and to stop the spread of ZIKV. This effort includes activities such as the use of insecticides, the elimination of stagnant water and educative public health campaigns (Bancroft et al. 2022), which are incorporated as η_1 in the epidemic model (35). Additionally, given that it has been noted that Zika can be transmitted sexually; condom use has been advised as a preventative measure. Brazil has also implemented a complete strategy for HIV prevention and care (Benzaken et al. 2019). This has involved administering ART to all HIV-positive individuals since 2013. Brazil started a campaign to distribute condoms, encouraging condom use among vulnerable populations. As a result, the number of deaths from AIDS in Brazil has significantly dropped (Bastos et al. 2009; Pereira et al. 2019).

Hence, we established the hypothetical scenario depicted in Figs. 5 and 6, the set of parameter values for which $\mathcal{R}_0 > 1$ (see Fig. 2) and initial conditions stated in Table 5 (population sizes for 2015). Specifically, we assume high probabilities of co-infection with $\omega_1 = 0.09$, $\omega_2 = 0.06$ and a recovery scale factor of $\epsilon = 0.1$. The balancing

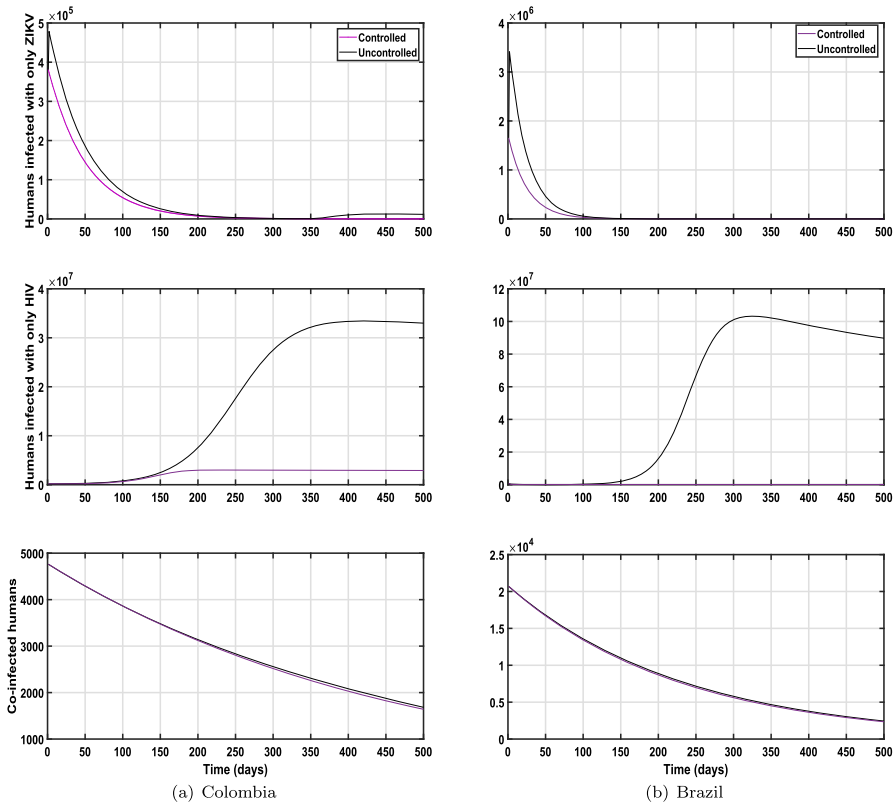


Fig. 8 Simulations of controlling infectious population in Colombia and Brazil (Color figure online)

parameter values were taken as $c_i = 0.5$ for $i = 1, \dots, 5$, and the weighting constant values were set as $d_i = 10^5$ for $i = 1, \dots, 3$. This scenario was chosen to illustrate the results of the control problem because it represents an extreme case where the basic reproductive number (\mathcal{R}_0) is greater than one, indicating an outbreak of the infections. This allows us to assess the effectiveness of control measures under conditions of high transmission and provides a robust test of the intervention strategies.

Figure 8 shows the behaviour of the infectious compartments I_z , I_h and I_{hz} from 2015 to mid-2016, with and without the implementation of the three control strategies. Overall, the implementation of the three control strategies is effective in reducing the load of infectious individuals in both countries. However, the reduction was more notable in individuals infected only with HIV. In the case of people infected only with ZIKV, there was a considerable reduction in the first 100 days of activation of the controls, which prevented the appearance of infection peaks in early 2015.

The number of people infected with HIV alone has been almost eliminated in Brazil, while in Colombia there has been a substantial reduction, although less spectacular than in Brazil. Patients infected with both HIV and ZikV were kept to minimal levels, as the size of this group naturally decreases, whatever the intervention, due to the limited number of individuals in this compartment.

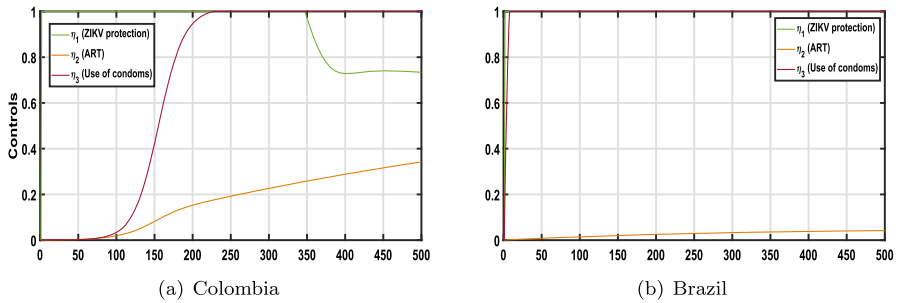


Fig. 9 Simulations of the behaviour of the controls in Colombia and Brazil (Color figure online)

It is interesting to observe the behaviour of the controls over the 500 days of their implementation (see Fig. 9). In both countries, the strategy that should remain almost 100% active throughout this period is the use of mosquito nets or repellents (protection against Zika). Another key strategy is the use of condoms, which must be maintained at a high level. By using condoms as the main sexual protection measure, the need for ART is reduced because it is more cost-effective to use condoms than to administer ART. Therefore, the implementation of the three controls proved to be an effective strategy to reduce the burden of Zika and HIV infections in Brazil and Colombia, with more pronounced results in HIV cases. The rapid decrease in Zika cases during the first 100 days of the measures highlighted the effectiveness of early control in preventing outbreaks. Controls are used for co-infected individuals in both countries, but due to their low prevalence, the impact of the strategies is less visible.

6 Discussion

The first documented cases of HIV/ZIKV co-infection in Colombia and Brazil in 2015 underscored the importance of investigating the interaction between these two viruses. The co-circulation of both viruses in the South American and Caribbean countries presented a significant burden for public health authorities. In this study, we used mathematical modelling to theoretically capture the transmission dynamics of co-infected individuals during the 2015 Zika outbreak in Colombia and Brazil. These findings were particularly relevant given the context of the Zika outbreak coinciding with a chronic HIV epidemic in those regions. Through a qualitative analysis and numerical simulations of our uncontrolled mathematical model, we found that Brazil had higher basic reproduction numbers compared to Colombia, which could be due to its significantly larger population size compared to Colombia. In both countries, the basic reproduction number associated with individuals infected only with HIV was higher than for those infected only with ZIKV, while the basic reproduction number for co-infected individuals was the lowest. The evidence indicates that controlling HIV outbreaks may be more complex than managing Zika outbreaks. This aligns with the fact that Zika transmission follows a seasonal pattern, whereas HIV remains persistent throughout the year. Additionally, the low basic reproduction number observed

for co-infected individuals is consistent with the limited number of co-infection cases reported in both countries during 2015. Using sensitivity indices of the basic reproductive number to parameters, it was found that for HIV transmission (\mathcal{R}_h), the most significant parameters were the rates of HIV transmission through sexual contact (β_h) and the average duration of the immunodeficiency period ($1/\sigma_1$). For Zika transmission (\mathcal{R}_z), the most important parameter was the mosquito mortality rate (μ_m). Regarding co-infection (\mathcal{R}_{hz}), the critical parameters were the rates of sexual transmission of Zika and HIV (β_z and β_h), and the average duration of the Zika infection ($1/\delta_z$). These results suggest that control strategies should focus on reducing the risk of sexual transmission and increasing mosquito mortality. Examination of actual cases of co-infection in Colombia and Brazil revealed that the probabilities of co-infection, ω_1 and ω_2 , were low, while the average duration of Zika infection ($1/\delta_z$) and the Zika recovery scaling factor (ϵ) remained stable. However, exploration of theoretical scenarios showed that increasing these probabilities led to an increase in the number of people co-infected.

Moreover, extending the duration of Zika infection increases the co-infection burden, implying that a longer Zika infection period increases the chances of HIV acquisition. Furthermore, reducing the scaling parameter ϵ , which denotes a slower Zika recovery in co-infected individuals, resulted in a substantial increase in co-infection cases. This suggests that these parameters, despite not significantly impacting the overall basic reproduction number (\mathcal{R}_0), could play a crucial role in various contexts. Consequently, it is essential to account for the variability of these parameters when investigating Zika and HIV co-infection dynamics, as critical values, such as $\epsilon < 0.2$, might cause a dramatic surge in co-infection cases, particularly when Zika infection lasts over 40 days in immunocompromised individuals.

Regarding the implementation of three control strategies: bed nets, ART, and the use of condoms, the study revealed that in both countries, the use of bed nets or repellents was crucial, requiring nearly 100% activation throughout, as it effectively prevented mosquito bites and was cost-efficient as a personal preventive measure. Additionally, condom use needed to be maintained at high levels, particularly in Brazil. In contrast, ART required less effort, as the use of condoms reduced the need for antiretroviral medication, making it a more cost-effective strategy. Implementation of the three controls effectively reduced the burden of Zika and HIV infections, with more significant results in HIV cases. The sharp decline in Zika cases within the first 100 days emphasized the importance of early control to prevent outbreaks. Although co-infected individuals were managed in both countries, their low prevalence made the impact of these strategies less visible.

Although this study has provided valuable information, it is crucial to recognize some limitations of its methodology. First, the study's reliance on numerical simulations with specific parameter values for Colombia and Brazil limits the generalization of the findings to other geographic locations. Different epidemiological landscapes, variable healthcare practices, and demographic differences between regions may result in distinct patterns of Zika and HIV co-infection dynamics. Second, this study's dependence on limited historical data and assumptions about intervention effectiveness may not fully capture the dynamic nature of evolving public health strategies. Current developments in medical interventions, changes in public health policies, and the emergence

of new viral variants can significantly affect the effectiveness of proposed intervention measures. These limitations emphasize the need for caution when extending the study findings. Further research is required to improve the applicability of mathematical models in different scenarios and challenges in terms of public health.

This study highlighted the need for ongoing research on ZIKV and HIV/AIDS transmission dynamics and the development of effective intervention strategies to control and prevent their spread. Future work in this field plans to incorporate compartments for women giving birth to babies with and without congenital malformations to better understand the impact of co-infection on children. Including these compartments would allow for a more detailed assessment of the long-term effects of co-infection on child health outcomes, including developmental delays, neurological deficits, and other complications. This approach could also facilitate the development of more specific prevention and treatment strategies for the affected children and their families. Ultimately, this research is crucial for improving our understanding of the complex interactions between HIV and Zika and for developing effective public health interventions to mitigate their impact on affected individuals and communities.

A Appendices

A.1 Proof of Lemma 1 item i.

From the definition of \mathcal{R}_z^* , we have that $\mathcal{R}_z^* = 2\mathcal{R}_{z_1} + \bar{\mathcal{R}}_{z_2} < 1$. This immediately implies that $2\mathcal{R}_{z_1} < 1$. Now, consider the alternate form of \mathcal{R}_z^* : $\mathcal{R}_z^* = \mathcal{R}_z^2 + 2\mathcal{R}_{z_1}(1 - \mathcal{R}_z)$. Given that $\mathcal{R}_z^* < 1$, we have $\mathcal{R}_z^2 + 2\mathcal{R}_{z_1}(1 - \mathcal{R}_z) < 1$. Rewriting the inequality, we get $\mathcal{R}_z(1 - 2\mathcal{R}_{z_1}) + 2\mathcal{R}_{z_1} < 1$.

Since $2\mathcal{R}_{z_1} < 1$, we can isolate \mathcal{R}_z as

$$\mathcal{R}_z(1 - 2\mathcal{R}_{z_1}) < 1 - 2\mathcal{R}_{z_1}.$$

Because $1 - 2\mathcal{R}_{z_1} > 0$, dividing both sides by $1 - 2\mathcal{R}_{z_1}$ yields $\mathcal{R}_z < 1$, which completes the proof.

A.2 Sensitivity index of \mathcal{R}_z with respect to β_z

We provide the derivative of \mathcal{R}_z with respect to β_z , denoted as $\frac{\partial \mathcal{R}_z}{\partial \beta_z}$, and subsequently computes the sensitivity index. We start with the expression for $\frac{\partial \mathcal{R}_z}{\partial \beta_z}$:

$$\begin{aligned} \frac{\partial \mathcal{R}_z}{\partial \beta_z} &= \frac{\partial}{\partial \beta_z} \left(\frac{\beta_z}{2\mu\kappa_1} + \sqrt{\left(\frac{\beta_z}{2\mu\kappa_1}\right)^2 + \frac{\alpha_m \beta_m \Lambda_m \mu}{\Lambda \mu_m^2 \kappa_1}} \right) \\ &= \frac{1}{2\mu(\delta_z + \mu + \mu_z)} + \frac{\beta_z}{4\mu^2(\delta_z + \mu + \mu_z)^2 \sqrt{\frac{\beta_z^2}{4\mu^2(\delta_z + \mu + \mu_z)^2} + \frac{\alpha_m \beta_m \Lambda_m \mu}{\Lambda \mu_m^2(\delta_z + \mu + \mu_z)}}}. \end{aligned}$$

After computing this derivative, we proceed to calculate the sensitivity index:

$$\frac{\partial \mathcal{R}_z}{\partial \beta_z} \frac{\beta_z}{\mathcal{R}_z} = \frac{\partial \mathcal{R}_z}{\partial \beta_z} \frac{\beta_z}{\mathcal{R}_z}.$$

This approach provides a quantitative measure of how \mathcal{R}_z responds to changes in β_z , considering its relationship with other parameters in the model.

A.3 Proof of Proposition 4

All state variables and controls are non-negative and, for $i = \{1, 2, 3\}$, the set of control variables $\eta_i \in \mathcal{A}$ is also convex and closed. We note that the boundedness of the optimal system (35) determines the compactness for the existence of the optimal control. Moreover, there exists a constant $\nu > 1$, $\omega_1 = \min(d_1, d_2, d_3)$, and $\omega_2 > 0$ such that

$$\mathcal{J}(\eta) \geq \omega_1 \|\eta\|^\nu - \omega_2. \tag{A.1}$$

Therefore, according to (Roxin and Lukes 1985), the controlled system (35) admits an optimal control solution η^* .

A.4 Proof of Proposition 5

We have

$$\begin{aligned} \frac{p_1}{dt} &= -\frac{\partial H}{\partial S} = p_1 \left[(1 - \eta_1)\tilde{\beta}_m + (1 - \eta_3)(\tilde{\beta}_c + \tilde{\beta}_z + \tilde{\beta}_h) + \mu \right] \\ &\quad - p_2 \left[(1 - \eta_1)\tilde{\beta}_m + (1 - \eta_3)\tilde{\beta}_z \right] \\ &\quad - p_3(1 - \eta_3)\tilde{\beta}_h - p_4(1 - \eta_3)\tilde{\beta}_c, \\ \frac{p_2}{dt} &= -\frac{\partial H}{\partial I_z} = -c_1 + p_1(1 - \eta_3)\frac{\beta_z}{N}S - p_2 \left[(1 - \eta_3)\frac{\beta_z}{N}S - \omega_2(1 - \eta_3)\tilde{\beta}_h - (\mu_z + \delta_z + \mu) \right] \\ &\quad - p_3 \left[\omega_1(1 - \eta_3)\beta_z \frac{I_h}{N} \right] \\ &\quad - p_4 \left[\omega_2(1 - \eta_3)\tilde{\beta}_h + \omega_1(1 - \eta_3)\frac{\beta_z}{N}I_h \right] \\ &\quad - p_6\delta_z + p_7(1 - \eta_1)\alpha_m \frac{S_m}{N} - p_8(1 - \eta_1)\alpha_m \frac{S_m}{N}, \\ \frac{p_3}{dt} &= -\frac{\partial H}{\partial I_h} = -c_2 + p_1(1 - \eta_3)\frac{\beta_h}{N}S + p_2\omega_2(1 - \eta_3)\frac{\beta_h}{N}I_z \\ &\quad - p_3 \left[(1 - \eta_3)\frac{\beta_h}{N}S - \omega_1[(1 - \eta_1)\tilde{\beta}_m + (1 - \eta_3)\tilde{\beta}_z] \right] \\ &\quad - (1 - \eta_2)\sigma_1 - \mu - p_4 \left[\omega_1[(1 - \eta_1)\tilde{\beta}_m + (1 - \eta_3)\tilde{\beta}_z] + \omega_2(1 - \eta_3)\frac{\beta_h}{N}I_z \right] \\ &\quad - p_5(1 - \eta_2)\sigma_1, \\ \frac{p_4}{dt} &= -\frac{\partial H}{\partial I_{hz}} = -c_3 + p_1(1 - \eta_3) \left(\frac{\beta_c\beta_h}{N} + \frac{\beta_z}{N} + \frac{\beta_h}{N} \right) S \end{aligned}$$

$$\begin{aligned}
 & -p_2 \left((1 - \eta_3) S \frac{\beta_z}{N} - \omega_2 (1 - \eta_3) \frac{\beta_h}{N} I_z \right) \\
 & -p_3 \left(\epsilon \delta_z + (1 - \eta_3) \frac{\beta_h}{N} S - \omega_1 (1 - \eta_3) \frac{\beta_z}{N} I_z \right) \\
 & +p_4 \left(\omega_2 (1 - \eta_3) \frac{\beta_h}{N} I_z + \omega_1 (1 - \eta_3) \frac{\beta_z}{N} I_z - \epsilon \delta_z + (1 - \eta_1) \sigma_2 + \mu_{hz} + \mu \right) \\
 & -p_5 (1 - \eta_2) \sigma_2 + p_7 (1 - \eta_1) \frac{\alpha_m}{N} S_m - p_8 (1 - \eta_1) \frac{\alpha_m}{N} S_m, \\
 \frac{p_5}{dt} &= -\frac{\partial H}{\partial A} = -c_5 + p_5 (\mu_h + \mu), \\
 \frac{p_6}{dt} &= -\frac{\partial H}{\partial R} = p_6 \mu, \\
 \frac{p_7}{dt} &= -\frac{\partial H}{\partial S_m} = p_7 ((1 - \eta_1) \tilde{\alpha}_m + \mu_m) - p_8 (1 - \eta_1) \tilde{\alpha}_m, \\
 \frac{p_8}{dt} &= -\frac{\partial H}{\partial I_m} = -c_4 + p_1 (1 - \eta_1) \frac{\beta_m}{N} S - p_2 (1 - \eta_1) \frac{\beta_m}{N} S \\
 & + p_3 \omega_1 (1 - \eta_1) \frac{\beta_m}{N} I_h - p_4 \omega_1 (1 - \eta_1) \frac{\beta_m}{N} I_h + p_8 \mu_m,
 \end{aligned}$$

with transversality conditions $p_i(T) = 0$, for $i = \{1, 2, 3, 4, 5, 6, 7, 8\}$. According to PMP, the optimal conditions are

$$\begin{aligned}
 \frac{\partial H}{\partial \eta_1} &= d_1 \eta_1 - (p_2 - p_1) \tilde{\beta}_m S + (p_4 - p_3) \omega_1 \tilde{\beta}_m I_h - (p_8 - p_7) \tilde{\alpha}_m S_m = 0, \\
 \frac{\partial H}{\partial \eta_2} &= d_2 \eta_2 - (p_5 - p_3) \sigma_1 I_h - (p_5 - p_4) \sigma_2 I_{hz} = 0, \\
 \frac{\partial H}{\partial \eta_3} &= d_3 \eta_3 - (p_2 - p_1) \tilde{\beta}_z S - (p_3 - p_1) \tilde{\beta}_h S - (p_4 - p_1) \tilde{\beta}_c S \\
 & - (p_4 - p_3) \omega_1 \tilde{\beta}_z I_h - (p_4 - p_2) \omega_2 \tilde{\beta}_h I_z = 0.
 \end{aligned}$$

Hence, we get assertions (5). This completes the proof.

Acknowledgements The authors appreciate the support provided by the One Health Modelling Network for Emerging Infections (OMNI-RÉUNIS) and Mathematics for Public Health (MfPH), which are financially supported by the Natural Sciences and Engineering Research Council of Canada (NSERC) and the Public Health Agency of Canada (PHAC).

Data Availability All data involved during this study are included in this published article.

Declarations

Conflict of interest Authors declare that have no conflict of interest to disclose in relation to this work.

References

Avusuglo WS, Bragazzi N, Asgary A, Orbinski J, Wu J, Kong JD (2023) Leveraging an epidemic-economic mathematical model to assess human responses to COVID-19 policies and disease progression. *Sci Rep* 13(1):12842

- Bancroft D, Power GM, Jones RT, Massad E, Iriat JB, Preet R, Kinsman J, Logan JG (2022) Vector control strategies in Brazil: a qualitative investigation into community knowledge, attitudes and perceptions following the 2015–2016 Zika virus epidemic. *BMJ Open* 12(1):e050991
- Bastos FIPM, Nunn A, Hacker MA, Malta M, Szwarcwald CL (2009) AIDS in Brazil: the challenge and the response. *Public health aspects of HIV/AIDS in low and middle income countries: epidemiology, prevention and care* 629–654
- Benzaken AS, Pereira GF, Costa L, Tanuri A, Santos AF, Soares MA (2019) Antiretroviral treatment, government policy and economy of HIV/AIDS in Brazil: is it time for HIV cure in the country?
- Bidokhti MR, Dutta D, Madduri LS, Woollard SM, Norgren R, Giavedoni L, Byrareddy SN (2018) SIV/SHIV-Zika co-infection does not alter disease pathogenesis in adult non-pregnant rhesus macaque model. *PLoS Negl Trop Dis* 12(10):e0006811
- Brasil P, Pereira JP, Moreira ME, Nogueira RMR, Damasceno L, Wakimoto M, Rabello RS, Valderramos SG, Halai U-A, Salles TS, Zin AA, Horovitz D, Daltro P, Boechat M, Gabaglia CR, de Sequeira PC, Pilotto JH, Medialdea-Carrera R, da Cunha DC, de Carvalho LMA, Pone M, Siqueira AM, Calvet GA, Baião AER, Neves ES, de Carvalho PRN, Hasue RH, Marschik PB, Einspieler C, Janzen C, Chery JD, de Filippis AMB, Nielsen-Saines K (2016) Zika virus infection in pregnant women in Rio de Janeiro. *New England J Med* 375:2321–2334
- “Brazil-piramide de población.” <https://datosmacro.expansion.com/demografia/poblacion/brasil>. Accessed: 02 Jan 2023
- Cao-Lormeau VM, Blake A, Mons S, Lastère S, Roche C, Vanhomwegen J, Dub T, Baudouin L, Teissier A, Larre P, Vial AL, Decam C, Choumet V, Halstead SK, Willison HJ, Musset L, Manuguerra JC, Despres P, Fournier E, Mallet HP, Musso D, Fontanet A, Neil J, Ghawché F (2016) Guillain-Barré syndrome outbreak associated with Zika virus infection in French Polynesia: a case-control study. *Lancet* 387(10027):1531–1539
- Castillo-Chavez C, Thieme HR (1994) Asymptotically autonomous epidemic models. *Science* 94
- Calvet G, Aguiar RS, Melo AS, Sampaio SA, De Filippis I, Fabri A, Araujo ES, de Sequeira PC, de Mendonça MC, de Oliveira L et al (2016) Guillain-Barré syndrome outbreak associated with Zika virus infection in French Polynesia: a case-control study. *Lancet Infect Dis* 16(6):653–660
- Chitnis N, Hyman JM, Cushing JM (2008) Determining important parameters in the spread of malaria through the sensitivity analysis of a mathematical model. *Bull Math Biol* 70:1272–1296
- “Colombia-piramide de población.” <https://datosmacro.expansion.com/demografia/estructura-poblacion/colombia>. Accessed: 02 Jan 2023
- Donoghoe MC et al (2006) Injecting drug use, harm reduction and HIV/AIDS. *HIV/AIDS in Europe: moving from death sentence to chronic disease management*, pp 43–66
- Driessche PVD, Watmough J (2002) Reproduction numbers and sub-threshold endemic equilibria for compartmental models of disease transmission. *Math Biosci* 180(1–2):29–48
- Forero-Martínez LJ, Murad R, Calderón-Jaramillo M, Rivillas-García JC (2020) Zika and women’s sexual and reproductive health: critical first steps to understand the role of gender in the Colombian epidemic. *Int J Gynecol Obstet* 148:15–19
- Galindo-Quintero J, Mueses-Marin HF, Montaña-Agudelo D, Pinzón-Fernández MV, Tello-Bolívar IC, Alvarado-Llano BE, Martínez-Cajas JL et al (2014) HIV testing and counselling in Colombia: local experience on two different recruitment strategies to better reach low socioeconomic status communities. *AIDS research and treatment* 2014
- Gao D, Lou Y, He D, Porco TC, Kuang Y, Chowell G, Ruan S (2016) Prevention and control of Zika as a mosquito-borne and sexually transmitted disease: a mathematical modeling analysis. Springer
- García PJ, Bayer A, Cárcamo CP (2014) The changing face of HIV in Latin America and the Caribbean. *Curr HIV/AIDS Rep* 11:146–157
- Gourinat AC, O’Connor O, Calvez E, Goarant C, Dupont-Rouzeyrol M (2015) Detection of Zika virus in urine. *Emerg Infect Dis* 21(1):98
- Grandits P, Kovacevic RM, Veliov VM (2019) Optimal control and the value of information for a stochastic epidemiological sis-model. *J Math Anal Appl* 476(2):665–695
- Hainzl J, Leko MD, Pignedoli A, Vrdoljak B (2022) 12: Ordinary differential equations and dynamical systems
- Heinisch M, Diaz-Quijano FA, Chiaravalloti-Neto F, Pancetti GM, Coelho RR, dos Santos Andrade P, Urbinatti PR, de Almeida RMMS, Lima-Camara TN (2019) Seasonal and spatial distribution of *Aedes aegypti* and *Aedes albopictus* in a municipal urban park in São Paulo, SP, Brazil. *Acta Tropica* 189:104–113

- João EC, da Ferreira OD, Gouvea MI, de Lourdes M, Teixeira B, Tanuri A, Higa LM, Costa DA, Mohana-Borges R, Arruda MB, Matos HJ, Cruz ML, Mendes-Silva W, Read JS (2018) Pregnant women co-infected with HIV and Zika: outcomes and birth defects in infants according to maternal symptomatology. *PLoS ONE* 13(7):e0200168
- Kabapy AF, Shatat HZ, El-Wahab EWA (2020) Attributes of HIV infection over decades (1982–2018): a systematic review and meta-analysis. *Transbound Emerg Dis* 67(6):2372–2388
- Khurshid Z, Zafar M, Khan E, Mali M, Latif M (2019) Human saliva can be a diagnostic tool for Zika virus detection. *J Infect Public Health* 12(5):601–604
- Koblischke M, Stiasny K, Aberle SW, Malafa S, Tsouchnikas G, Schwaiger J, Kundi M, Heinz FX, Aberle JH (2018) Structural influence on the dominance of virus-specific CD4+T cell epitopes in Zika virus infection. *Front Immunol* 9:366429
- Machado-Silva A, Guindalini C, Fonseca FL, Pereira-Silva MV, Fonseca BDP (2019) Scientific and technological contributions of Latin America and Caribbean countries to the Zika virus outbreak. *BMC Public Health* 19:1–11
- McCluskey CC, Muldowney JS (1998) Bendixson-Dulac criteria for difference equations. *J Dyn Differ Equ* 10:567–575
- Mittal R, Nguyen D, Debs LH, Patel AP, Liu G, Jhaveri VM, Kay S-IS, Mittal J, Bandstra ES, Younis RT et al (2017) Zika virus: an emerging global health threat. *Front Cell Infect Microbiol* 7:486
- Mlakar J, Korva M, Tul N, Popović M, Poljšak-Prijatelj M, Mraz J, Kolenc M, Rus KR, Vipotnik TV, Vodusek VF, Vizjak A, Pižem J, Petrovec M, Županc TA (2016) Zika virus associated with microcephaly. *New England J Med*, 374
- Oehler E, Watrin L, Larre P, Leparç-Goffart I, Lastãre S, Valour F, Baudouin L, Mallet HP, Musso D, Ghawche F (2014) Zika virus infection complicated by Guillain-Barré syndrome—case report, French Polynesia, December 2013. *Eurosurveillance* 19
- Patterson J, Sammon M, Garg M (2016) Dengue, Zika and chikungunya: emerging arboviruses in the New World. *West J Emerg Med* 17(6):671–679. <https://doi.org/10.5811/westjem.2016.9.30904>
- Pereira GFM, Sabidó M, Caruso A, Benzaken AS (2019) Decline in reported AIDS cases in Brazil after implementation of the test and treat initiative. *BMC Infect Dis* 19:1–8
- Pontryagin LS, Boltyanskii V, Gamkrelidze R, Mishchenko E, Tirogoff K, Neustadt L (2018) *LS Pontryagin selected works: the mathematical theory of optimal processes*. Routledge
- Prieto K, Romero-Leiton JP (2021) Current forecast of HIV/AIDS using Bayesian inference. *Nat Resour Model* 34(4):e12332
- Romero-Leiton JP, Castellanos JE, Ibagüen-Mondragón E (2019) An optimal control problem and cost-effectiveness analysis of malaria disease with vertical transmission applied to San Andrés de Tumaco (Colombia). *Comput Appl Math* 38:1–24
- Rothan HA, Bidokhti MR, Byrareddy SN (2018) Current concerns and perspectives on Zika virus co-infection with arboviruses and HIV. *J Autoimmun* 89:11–20
- Roxin E, Lukes DL (1985) *Differential equations: classical to controlled*. The American Mathematical Monthly 92
- Saltelli A, Ratto M, Andres T, Campolongo F, Cariboni J, Gatelli D, Saisana M, Tarantola S (2008) *Global sensitivity analysis: the primer*. John Wiley & Sons
- Smith DW, Mackenzie J (2016) Comment: Zika virus and Guillain-Barré syndrome: another viral cause to add to the list
- Tilton JC, Doms RW (2010) Entry inhibitors in the treatment of HIV-1 infection. *Antiviral Res* 85(1):91–100
- Villamil-Gómez WE, Sánchez-Herrera Álvaro Rosendo, Hernández-Prado H, Hernández-Iriarte J, Díaz-Ricardo K, Vergara-Serpa O, Castellanos J, Portela-Gaviria JE, Patiño-Valencia S, Vargas-Bedoya DC, Orozco-Villa AF, Reyes-Guerrero SS, Castrillón-Spitia JD, Murillo-García DR, Henao-SanMartin V, Londoño JJ, Bedoya-Rendón H, de Jesús Cárdenas-Pérez J, Cardona-Ospina JA, Lagos-Grisales GJ, Rodríguez-Morales AJ (2018) Zika virus and HIV co-infection in five patients from two areas of Colombia
- Zika strategic response plan quarterly update. <https://www.who.int/publications/i/item/WHO-ZIKV-SRF-16.4>. Accessed:2023-04-05

Springer Nature or its licensor (e.g. a society or other partner) holds exclusive rights to this article under a publishing agreement with the author(s) or other rightsholder(s); author self-archiving of the accepted manuscript version of this article is solely governed by the terms of such publishing agreement and applicable law.